---

**Article:**
Zoulias, N., Rowe, J., Thomson, E.E. orcid.org/0000-0002-0266-7090 et al. (8 more authors) (2021) Inhibition of Arabidopsis stomatal development by plastoquinone oxidation. Current Biology, 31 (24). 5622-5632.e7. ISSN 0960-9822

https://doi.org/10.1016/j.cub.2021.10.018

---

# Inhibition of *Arabidopsis* stomatal development by plastoquinone oxidation

Nicholas Zoulias,[1] James Rowe,[2] Emma E. Thomson,[1] Magdalena Dabrowska,[1] Holly Sutherland,[1] Gustaf E. Degen,[1] Matthew P. Johnson,[1] Svetlana E. Sedelnikova,[1] Georgia E. Hulmes,[1] Ewald H. Hettema,[1] and Stuart A. Casson[1, 3, 4]

[1] Department of Molecular Biology and Biotechnology, University of Sheffield, Sheffield, UK

[2] Sainsbury Laboratory, University of Cambridge, 47 Bateman Street, Cambridge, UK

[3] Lead Contact: s.casson@sheffield.ac.uk

[4] Twitter: @casson_stuart

## SUMMARY

Stomata are the pores in the epidermal surface of plant leaves that regulate the exchange of water and $CO_2$ with the environment thus controlling leaf gas exchange.[1] In the model dicot plant Arabidopsis thaliana, the transcription factors SPEECHLESS (SPCH) and MUTE sequentially control formative divisions in the stomatal lineage by forming heterodimers with ICE1.[2] SPCH regulates entry into the stomatal lineage and its stability or activity is regulated by a mitogen-activated protein kinase (MAPK) signalling cascade, mediated by its interaction with ICE1.[3-6] This MAPK pathway is regulated by extracellular EPIDERMAL PATTERNING FACTOR (EPFs) peptides, which bind a transmembrane receptor complex to inhibit (EPF1 and EPF2) or promote (STOMAGEN/EPFL9) stomatal development.[7-9] MUTE controls the transition to guard mother cell (GMC) identity and is regulated by the HD-ZIP transcription factor HDG2, which is expressed exclusively in stomatal lineage cells.[10, 11] Light signals acting through phytochrome and cryptochrome photoreceptors positively regulate stomatal development in response to increased irradiance.[12, 13] Here we report that stomatal development is also regulated by the redox state of the photosynthetic electron transport chain (PETC). Oxidation of the plastoquinone (PQ) pool inhibits stomatal development by negatively regulating SPCH and *MUTE* expression. This mechanism is dependent on MPK6 and forms part of the response to lowering irradiance, which is distinct to the photoreceptor dependent response to increasing irradiance. Our results show that environmental signals can act through the PETC, demonstrating that photosynthetic signals regulate the development of the pores through which CO2 enters the leaf.



## KEYWORD

Stomata, chloroplast, development


## RESULTS

Previous work has shown that the red light photoreceptor phyB is the foremost photoreceptor required for light mediated control of the stomatal developmental pathway (Figure S1A) and at higher growth irradiances *phyB* mutants have a reduced stomatal index (SI; the proportion of cells in the epidermis that are stomata).[12] To investigate whether phyB controls the expression of major regulators of stomatal development under dynamic light conditions, we exposed seedlings of both wild-type (WT; Col-0) and *phyB* null mutants to light shift experiments and then performed quantitative RT-PCR analyses. A 6h light shift resulted in robust changes in stomatal gene expression in WT seedlings exposed to either an increase (50 µmol $m^{-2}$ $s^{-1}$ to 250 µmol $m^{-2}$ $s^{-1}$) or a decrease (250 µmol $m^{-2}$ $s^{-1}$ to 50 µmol $m^{-2}$ $s^{-1}$) in irradiance, when

compared to their respective controls (Figures 1A and 1B). The observed gene expression changes, particularly those of *SPCH* and *MUTE*, correlate with the differences seen in SI when seedlings are grown under these steady state irradiances (Figure S1B). Significantly, *phyB* mutants appeared insensitive to dynamic increases in irradiance (50-250) but had a similar response to WT seedlings when exposed to a decrease in irradiance (250-50) (Figures 1A and 1B). The blue light perceiving cryptochromes (CRYs) also regulate stomatal development,[13] so we next examined whether *cry1cry2* mutants, which are defective in the two main CRY photoreceptors, regulate these changes in stomatal gene expression to a decrease in irradiance but found that they also respond in a WT manner, as did a *phyBcry1cry2* triple mutant (Figure S1C-F). Whilst we cannot fully discount that photoreceptors redundantly control a response to decreased irradiance, our data suggests that other signalling pathways may also be required to regulate this response.

**Plastoquinone oxidation regulates stomatal development**

If the main photoreceptors do not fully account for the changes in gene expression we detected in response to a decrease in irradiance, we considered other mechanisms through which light can mediate plant responses. Light is the major regulator of PETC and in particular, the redox status of the PQ pool, which carries electrons from photosystem II (PSII) to cytochrome b6f (cyt$b_6f$). Previous studies have shown that the PQ redox state regulates developmental processes such as growth form, flowering and splicing.[14-17] A reduction in irradiance results in a decreased electron transfer rate from PSII to the PQ pool, leading to its oxidation, which can be measured via the chlorophyll fluorescence parameter 1-qP (Figure 1 C, D and S1G). Oxidation of the PQ pool can also be achieved by treatment with DCMU [3-(3,4-dichlophenyl)1,1-dimethylurea], a specific inhibitor of PSII.[18] Treatment of 3 d.p.g. (days post germination) and 7 d.p.g. seedlings resulted in rapid and robust oxidation of the PQ pool (Figure 1 C and D). To test whether oxidation of the PQ pool affects stomatal development, 3 d.p.g. seedlings were sprayed with 10μM DCMU and epidermal impressions were taken daily in order to determine the cotyledon stomatal index (SI); this single spray treatment does not cause seedling death or affect cotyledon growth (Figure 1E and S1H). The SI of the DCMU treated seedlings was significantly reduced compared to mock-sprayed controls at both 48h and 72h post-treatment, whereas the effect on density was more minor (Figure 1F and 1G). As cotyledon size is also not affected, this suggests that DCMU has increased epidermal cell divisions and that despite the reduced probability of a cell becoming a stomata, this can compensate to allow an equitable SD. Such compensation has been previously observed during leaf development when cell division is

perturbed.[19] The reduced SI is similar to that observed when plants are grown under low versus higher irradiances (Figure S1B),[12] suggesting that oxidation of the PQ pool may negatively regulate stomatal development. We next utilised qRT-PCR to examine the expression of key regulators of the stomatal developmental pathway. Significantly, *SPCH* and *MUTE* showed robust reductions in expression within 6h of treatment with DCMU (Figure 1H, Dataset S1). Expression of ICE1 was also downregulated (Figure 1H, Dataset S1). However, FAMA, which regulates the final step in stomatal development,[20] was not affected (Figure 1H, Dataset S1). The magnitude of these changes in gene expression, are comparable to those observed following the dynamic (250-50) changes in irradiance (Figure S1I, Dataset S1). This suggests that the observed reductions in SI following DCMU treatment may be due to targeting of the early steps of stomatal development regulated by SPCH and MUTE.

We next wished to assess whether this change was specifically associated with the redox status of the PQ pool, or other aspects of chloroplast function. We first treated seedlings with norflurazon, which inhibits carotenoid biosynthesis resulting in oxidative destruction of chloroplasts.[21] In contrast to DCMU, norflurazon treatment did not affect the expression of these transcription factors (Figure S1J). We next examined the response of seedlings to treatment with the inhibitor 2,5-dibromo-3-methyl-6-isopropylbenzoquinone (DBMIB), which causes reduction of the PQ pool mimicking an increase in irradiance.[18] In contrast to DCMU, seedlings grown in the presence of DBIMB had a significantly increased SI compared to controls (Figure S1B), although the impact on the PQ pool was minimal at the end of the treatment (Figure S1K). Notably, treatment with DBMIB altered expression of *STOMAGEN* (*STOM*), as opposed to *SPCH* and *MUTE* (Figure S1L), though the treatment methods for DCMU and DBMIB are different and so are not directly comparable. We next examined stomatal development in mutant lines that have been shown to have perturbations in PETC. The *serine/threonine-protein kinase 7* (*stn7*) and *thylakoid-associated phosphatase 38* (*tap38*) have both been shown to regulate PETC under dynamic light conditions by regulating state transitions and thylakoid stacking.[22-24] We found that growth under high light conditions had a consistent trend ($P < 0.1$) of a reduced SI compared to Col-0 (Figure S1M). This is indicative of the PETC influencing stomatal development even whilst under constant conditions. Far-red light has often been used to manipulate the redox status of the PETC because it preferentially excites PSI leading to net oxidation of the PQ pool.[25] Therefore, to manipulate the redox status of the PETC independently of DCMU and the *phytochromes,* the phytochrome deficient *phyQ* mutant was subjected to a light transfer from 250 µmol $m^{-2}$ $s^{-1}$ of white light to 50 µmol $m^{-2}$ $s^{-1}$ of far-red light.[26] Gene expression analysis indicated that, similar to DCMU treatment, manipulation of PETC with far-

red light was able to regulate *SPCH* and *MUTE* and that this response is not dependent on the red/far-red perceiving *phytochromes* (Figure S1N). Taken together, these data show that perturbations in chloroplast function are not responsible for the changes in stomatal development and these effects may be specific to the redox status of the PETC.

**Oxidation of plastoquinone impacts SPEECHLESS and MUTE protein levels**

To examine whether oxidising the PQ pool regulates the cellular protein levels of SPCH and MUTE, we used confocal microscopy to analyse lines expressing $SPCH_{pro}$*:SPCH-GFP* [3] and $MUTE_{pro}$*:MUTE-GFP* transgenes. Within individual cells, DCMU treatment caused significant reductions in SPCH and MUTE protein levels (Figures 2A, 2B and S2A). Statistical analysis of the $SPCH_{pro}$*:SPCH-GFP* and $MUTE_{pro}$*:MUTE-GFP* lines also demonstrated that fewer cells than expected express SPCH or MUTE after DCMU treatment, though this was only highly significant for SPCH (two-sided Chi-Square SPCH, p-value <0.0001; MUTE p-value <0.1, Dataset S1). Given that DCMU caused reductions in SPCH, we hypothesised that increasing SPCH stability or activity would alter sensitivity to DCMU. A transgenic line expressing a phosphomutant version of SPCH (SPCH1-4A), mutated in residues targeted by MPK3/6, shows increased stability and activity.[4] SPCH1-4A cotyledons showed a reduced SI because stabilising SPCH enhances production of stomatal lineage cells and inhibits their progression to later stages of stomatal development. We observed no difference in the SI of SPCH1-4A cotyledons following mock and DCMU treatments (Figure 2C). The SPCH1-4A variant is translationally fused to YFP so we quantified the impact of DCMU treatment on cellular protein levels of SPCH-GFP and SPCH1-4A-YFP and found that protein levels of SPCH1-4A-YFP are not affected by DCMU, in contrast to SPCH-GFP (Figures 2D, 2E and S2B). Furthermore, qRT-PCR analysis showed that stabilising SPCH also reduced sensitivity to DCMU at the level of gene expression, including the direct SPCH target *EPF2* (Figure 2F).[27] Together these data suggest that oxidation of the PQ pool negatively controls stomatal development by regulating both the transcription and the stability/activity of SPCH and MUTE. In the case of SPCH, this regulation may occur via a MAPK signalling pathway given that the SPCH1-4 variant is mutated in MPK3/6 targeted residues.

**Non-canonical activation of MPK6 following plastoquinone oxidation**

The EPFs regulate stomatal developmental by binding to a receptor complex that in turn controls the activity of the MAPK signalling pathway that targets SPCH and other steps in the stomatal developmental pathway.[7-9] EPF1 and EPF2 activate the MAPK pathway and negatively

regulate stomatal development whereas STOM suppresses the MAPK signalling cascade. We examined the expression of these EPFs by qRT-PCR and found that *EPF2* expression, but not *EPF1* or *STOM*, was reduced by DCMU treatment (Figure S3A). As a negative regulator of stomatal development the reduction in *EPF2* expression does not correlate with the negative regulation of stomatal development by DCMU treatment. However, *EPF2* is a direct target of SPCH,[27] whereas *EPF1* and *STOM* are not, which may explain this result. This is further supported by the downregulation of *BASL*, another direct SPCH target,[27] after DCMU treatment (Figure S3A). A high light to low light transfer also shows a similar negative regulation of *BASL* and *EPF2* suggesting that DCMU treatment partially mimics this high to low light transfer (Figure S3B).

STOM positively regulates stomatal development and unlike *EPF1* and *EPF2*, which are restricted to the epidermis, is expressed in the inner mesophyll tissue.[9] Mesophyll expression has led to the hypothesis that STOM may provide a mechanism through which photosynthetic tissue can regulate stomatal development.[9] However, we found that DCMU has no major impact on the expression of *STOM*, as determined by qRT-PCR (Figure S3A). To determine whether STOM regulates sensitivity to DCMU we analysed plants overexpressing *STOM* (STOM OE).[28] These plants produce significantly more stomata because the increased levels of STOM compete with EPF1/EPF2 and inactivate the MAPK signalling cascade. Although STOM OE seedlings have a significantly increased SI compared to WT plants, they responded to DCMU treatment with a reduction in SI that was proportional to a WT response. The SI of DCMU treated Col-0 was 89.6% (SEM: 2.1%), whilst STOM OE was 91.3% (SEM: 3.2%) of their respective controls (Figure 3A). qRT-PCR also demonstrated that the STOM OE retained WT-like sensitivity to DCMU, particularly with regards SPCH expression (Figure 3B). We also investigated whether the major receptor of the EPFs and STOM, *ERECTA,* was involved in the signalling pathway and found that the *erecta* mutant maintained WT-like sensitivity to DCMU (Figure S3C). Our evidence suggests that STOM, as well as EPF1 and EPF2, are not major components of the pathway activated in response to oxidation of the PQ pool. Indeed, taken together our data would suggest that chloroplast signals, generated in response to oxidation of the PQ pool, do not primarily function via an EPF mediated pathway. STOM expression was upregulated by DBMIB treatment (Figure S1L) so it is plausible that reduction of the PQ pool targets the stomatal developmental pathway differently to when the PQ pool is oxidised.

The question therefore arises as to whether this chloroplast pathway requires inter-tissue or even intercellular signals? Most chloroplasts are found in mesophyll tissue and the mature

epidermis lacks chloroplasts (except in guard cells). However, analysis of developing cotyledons, via chlorophyll fluorescence, clearly revealed the presence of chloroplasts throughout the immature epidermis including stomatal lineage cells expressing SPCH and MUTE (Figure S2C). Lambda scans of 5nm (SPCH-GFP) or 10nm (MUTE-GFP) bandwidth were used to verify that chloroplast fluorescence in the stomatal lineage occurred at 680nm, the emission peak for PSII-associated chlorophyll. This is in line with other studies, which have shown that early in development, the epidermis does contain functional chloroplasts. [29] This indicates that chloroplast derived signals from the epidermis may have the potential and be sufficient to regulate the stomatal developmental pathway, but further experimentation is required to address this possibility.

The fact that stabilising SPCH by mutating MPK3/6 phosphorylation sites reduces sensitivity to DCMU led us to next examine the role of MAP kinases in this mechanism. DCMU treatment resulted in a modest but significant increase in *MPK6* expression but no change in *MPK3* (Figure S3D). We therefore examined what impact DCMU treatment had on activation of MPK3/6 using antibodies specific to the active versions of these kinases. MPK6 and MPK3 were rapidly activated following DCMU treatments, though MPK3 activation appeared less abundant as determined by this assay (Figures 3C, and S3E). Given that DCMU was activating MPK6 most strongly, we next examined stomatal development in the *mpk6* mutant and found that *mpk6* mutants are insensitive to DCMU treatment (Figure 3D), though it is likely that MPK3 and MPK6 have overlapping functions and there may be some redundancy. At the level of gene expression, the *mpk6* mutant was less responsive to the DMCU treatment, with no significant change in expression of *SPCH* and *MUTE*, nor of the SPCH target *EPF2* (Figure 3E). This supports a mechanism whereby changes in the redox status of the PETC regulate MPK6 activity. In the context of stomatal development, MPK6 acts downstream of the EPF-Receptor-MAPK module, and yet our earlier data indicates that this mechanism is likely independent of the EPFs indicating that oxidation of the PQ pool activates MPK3/6 by an alternative mechanism. Reactive oxygen species (ROS) have been shown to activate MPK3/6 and treatment with some photosynthetic inhibitors can induce ROS, though previous studies showed that DCMU does not.[30, 31] To test the potential generation of ROS as the signalling intermediate following treatment with DCMU, we quantified $H_2O_2$ (Figure S3F). We found that there was no generation of ROS following treatment with DCMU and this is further reflected by the gene expression response of ROS responsive genes (Figures S3F and S3G). We also investigated whether the photosynthesis-associated nuclear genes (*PhANGs*) were being modulated following treatment with DCMU as this might indicate the chloroplast signals were modulating

light signalling components.[32] The *PhANGs* showed no consistent trend suggesting that the co-opting of light signalling pathways was unlikely (Figure S3H). It has previously been demonstrated that chloroplast signals can activate MPK6 via the chloroplast CALCIUM SENSING RECEPTOR, CAS, whilst the CHLOROPLAST SENSOR KINASE, CSK, regulates chloroplastic genes in response to redox signals.[33, 34] However, both *cas* and *csk* mutants still showed downregulation of *SPCH* and its targets as well as *MUTE* following DCMU treatment (Figures S3I and S3J). *cas* mutants show either delayed or reduced activation of MPK6 in response to chloroplast signals,[33] which may explain our results, though we cannot exclude that these or other factors act redundantly in this chloroplast mediated signalling pathway.

Whilst MPK6 can target SPCH protein via ICE1,[6] which accounts for a reduction in cells entering the stomatal lineage, the question remained as to how oxidation of the PQ pool results in downregulation of both *SPCH* and *MUTE* transcript levels, as observed in our qRT-PCR analyses. *SPCH* is transcriptionally regulated by PIF4 under elevated temperature,[35] however both *SPCH* expression and its *target, EPF2*, are downregulated in a *pif4* mutant treated with DCMU, indicating that PIF4 is not involved in this pathway (Figure S3K). SPCH has the potential to regulate its' own expression,[27] so we cannot discount SPCH autoregulation as a mechanism.

**MPK6 phosphorylation of HDG2 regulates stomatal development**

MUTE also forms a major checkpoint in stomatal development and so we next investigated control of this point of the pathway. It is not clear from the literature whether SPCH directly regulates *MUTE* expression; ChIP analysis has shown that SPCH can bind the MUTE promoter but data from the same study, using an inducible SPCH1-4A line, showed no regulation of *MUTE* by SPCH.[27] Using a dual luciferase system, we observed a slight decrease in expression of the *MUTEproLUC* reporter in the presence of SPCH and we did not observe auto-activation of the *MUTEproLUC* construct by MUTE (Figure 3F). Using plants containing an inducible *SPCH* construct, *MUTE* was also found to not be regulated directly by *SPCH* although the direct targets *EPF2* and *BASL* were significantly regulated (Figure S3L). *MUTE* is directly regulated by the epidermal specific HD-ZIP transcription factor HDG2, which is expressed in early stomatal lineage cells that express SPCH and MUTE.[11] We therefore examined the response of *hdg2* mutants to DCMU treatment and found that at both the developmental level and molecular level, *hdg2* mutants were less responsive to this treatment, with no change in SI and no change in *SPCH* or *MUTE* expression (Figures 4A and 4B). The fact that *SPCH* expression in *hdg2* mutants showed reduced sensitivity to DCMU suggests it may regulate *SPCH* expression. This was supported by dual luciferase assays in which we observed activation of a *SPCHproLUC*

reporter by HDG2 (Figure 4C), as well as EMSA data which indicates HDG2 can bind to the *SPCH* promoter (Figure S4A). The SPCH target *EPF2* was still downregulated in *hdg2* mutants, which would suggest that MPK6 targeting of SPCH was still functional (Figure 4A). From this, we concluded that HDG2 is likely to be a component of this chloroplast pathway but little is known about regulation of this transcription factor. Using high light to low light transfers, we compared the response of *mpk6* and *atml1hdg2* to that of wild type (Figure S4B and C). *atml1hdg2* was used to try and eliminate some of the redundancy between the epidermally expressed class IV HD-Zips.[11] We found that following a transfer to low light, the *atmlhdg2* mutant had a non-significant reduction of *SPCH* whereas SPCH was significantly reduced in Wild type. *atml1hdg2* also had an increase in *MUTE* expression rather than the decrease seen in the Wild-type (Figure S4B). Whereas, *mpk6* had a relatively wild-type response to the light transfer which might in part be due to redundancy between *MPK6* and *MPK3* (Figure S4C).

Expression of *HDG2* was not altered by DCMU treatment (Figure S4D) however, this does not discount a post-translational mechanism of regulation. HDG2, as well as other epidermally expressed HD-Zips, regulates the expression of genes containing L1 boxes.[36] We therefore examined the expression of these L1 box genes as a proxy for HDG2 activity and found that in general their expression is downregulated following DCMU treatment (Figure S4D), supporting a mechanism in which HDG2 abundance and/or activity is regulated by oxidation of the PQ pool. Given that MPK6 can regulate SPCH and ICE1,[4, 6, 37] we therefore asked whether MPK6 has a role in regulating HDG2 function using the dual luciferase reporter system. HDG2 was able to significantly upregulate the luciferase reporter of both *SPCHproLUC* and *MUTEproLUC* constructs when co-expressed in protoplasts (Figures 4C and 4D). Addition of MPK6 to the system significantly reduced the transcriptional activation of both of these by HDG2 (Figures 4C and 4D), suggesting that MPK6 either targets HDG2 activity or its ability to bind the *SPCH* and *MUTE* promoters. We therefore analysed the expression of the L1 box containing genes in *mpk6* mutants following DCMU treatment and found that unlike in the WT control, their expression did not change in the *mpk6* mutant (Figure S4E). Together, these data support a role for MPK6 in regulating activity of HDG2 leading us to next examine a potential interaction between these two factors. We were able to detect an interaction between MPK6 and HDG2 with an *in vitro* binding assays using recombinant tagged MPK6 and HDG2 (Figure 4E and S4G). This interaction between MPK6 and HDG2 was confirmed, using a yeast two-hybrid system (Figure S4F). To investigate whether the interaction between MPK6 and HDG2 lead to the phosphorylation of HDG2 we performed *in vitro* kinase assays using recombinantly expressed proteins. *In vitro* kinase assays show that the MBP-HDG2 is phosphorylated by

MPK6, whereas MBP only is not (Figure 4F and S4G). This data, together with the mutant analysis and reporter assays supports a novel role for MPK6 in regulating HDG2 activity. MPK6, activated following oxidation of the PQ pool is therefore able to modulate decisions within the stomatal lineage by targeting SPCH, as well as HDG2, which is required for correct expression of *MUTE* and potentially *SPCH* (Figure S4H). The dual regulation of SPCH and *MUTE* via direct and indirect interactions of MPK6 respectively, further exemplifies the developmental plasticity of the stomatal lineage and how environmental signals can influence outcomes at different stages beyond entry into the lineage.

## Discussion

Environmental signals have long been known to regulate stomatal development and it has been demonstrated that light signals regulate these pathways through photoreceptor signalling pathways. However, photoreceptor signalling does not readily account for all aspects of light mediated stomatal development, in particular changes that occur in response to a decrease in irradiance. Significantly, given the role of stomata in $CO_2$ uptake, there has been no direct link between their development and photosynthetic performance. Here we show that chloroplast signals acting through MPK6, regulate core transcription factors to control key steps in the stomatal developmental pathway and builds on a growing body of evidence that chloroplasts are environmental sensors.[14-16, 38] This pathway is stimulated by oxidation of the PQ pool, though we also provide evidence that reduction of the PQ pool positively regulates stomatal development suggesting there are alternative pathways, which may be independent or acting in conjunction with the photoreceptors and can positively regulate stomatal development. Oxidation of the PQ pool can occur at low light, increased temperature and potentially an increased concentration of terminal electron acceptors, such as $CO_2$.[39] Such conditions are known to negatively regulate stomatal development.[12, 33, 40] Further, this chloroplast pathway could reconcile the observation that increased irradiance and [$CO_2$], which both positively affect assimilation rates, have opposing effects on stomatal development, as these conditions can have opposing impacts on the PQ redox state. This pathway may therefore enable plants to use photosynthetic activity and in conjunction with photoreceptor signalling, rapidly integrate multiple signals to mediate developmental outcomes. The fact that the stomatal lineage is asynchronous with cells at different stages of development at any given time means that signals could act at this local level to influence a cell's development trajectory. It is possible that accumulation or dynamic changes in post-translational modifications within such windows of time, may determine the activity of SPCH, MUTE or HDG2 and ultimately the cell fate decision. Further understanding of these

integrative processes will provide us with additional tools to manipulate leaf gas exchange capabilities to improve resource use and understand the impacts of future climate change on this trait.


## ACKNOWLEDGEMENTS

We would like to thank Julie Gray and Piers Hemsley for discussing the work and materials and Dominique Bergmann, Roger Hellens, John Clark Lagarias and the Nottingham Arabidopsis Stock Centre for kindly providing materials. This work was funded by the Biotechnology and Biological Sciences Research Council (BBSRC) grant to SAC (BB/N002393/1) and a BBSRC Studentship to MD (BB/M011151/1).


## AUTHOR CONTRIBUTIONS

Conceptualization, S.A.C. and N.Z; Methodology, N.Z., J.R, and S.A.C.; Investigation, N.Z., J.R, M.D., H.S., G.H., E.E.T., G.E.D., S.S., and S.A.C.; Writing – Original Draft, S.A.C.; N.Z. and J.R.; Funding Acquisition, S.A.C.; Supervision, E.H.H., M.P.J., E.E.T., and S.A.C.

## DECLARATION OF INTERESTS

The authors declare no competing interests

## FIGURE LEGENDS

**Figure 1: Oxidation of the PQ pool inhibits stomatal development.**

**A,** Expression levels of transcription factor regulators of stomatal development (*SPCH*, *MUTE*, *FAMA*, *ICE1*) examined by qRT-PCR, 6h post light transfer (50 µmol $m^{-2}$ $s^{-1}$ to 250 µmol $m^{-2}$ $s^{-1}$), in Col-0 and *phyB* backgrounds**.** The expression of UBC21 served as internal control. The error bars indicate the SEM (n = 3 biologically independent samples). Two-Tailed T-Tests (assuming unequal variance) were performed on each gene tested between mock and light transfer treatments in the same genetic background (p values are indicated by *; * < 0.05). See also Figures S1C and S1E.

**B,** Expression levels of transcription factor regulators of stomatal development (*SPCH*, *MUTE*, *FAMA*, *ICE1*) examined by qRT-PCR, 6h post light transfer (250 µmol $m^{-2}$ $s^{-1}$ to 50 µmol $m^{-2}$ $s^{-1}$), in Col-0 and *phyB* backgrounds**.** The expression of UBC21 served as internal control. Figure 1B and S1F were performed as a single experiment. The error bars indicate the SEM (n = 3 biologically independent samples). Two-Tailed T-Tests (assuming unequal variance) were

performed on each gene tested between mock and light transfer treatments in the same genetic background (p values are indicated by * and ***. * < 0.05; *** < 0.001). See also Figures S1D and S1F.

**C,** Excitation pressure (1-qP) plotted against time following a single mock or 10 μM DCMU treatment of 3 d.p.g. Col-0 plants. N=3 independent plants per treatment and error bars indicate SEM.

**D,** Excitation pressure (1-qP) plotted against time following a single mock or 10 μM DCMU treatment of 7 d.p.g. Col-0 plants. N=3 independent plants per treatment and error bars indicate SEM.

**E,** 3 d.p.g. seedlings were treated with mock or 10 μM DCMU and imaged 6 d.p.g. demonstrating no lethality due to the DCMU treatment. Scale bars are 5 mm in length. Quantification of cotyledon area supports no difference in growth rate (Fig. S1H)

**F,** Stomatal Index of cotyledons following a single mock or 10 μM DCMU treatment started 3 d.p.g. and continued for 72h. Epidermal counts taken from at least 36 cotyledons from >18 independent plants per time point. Two-Tailed T-Tests (assuming unequal variance) were performed on each time point between mock and DCMU treatments. 48 hours P=0.0431, 72 hours P= 0.000286.

**G,** Stomatal Density of cotyledons following a single mock or 10 μM DCMU treatment started 3 d.p.g. and continued for 72h. Epidermal counts taken from at least 36 cotyledons from >18 independent plants per timepoint. Two-Tailed T-Tests (assuming unequal variance) were performed on each time point between mock and DCMU treatments. 48 hours P=0.0431, 72 hours P= 0.000286.

**H,** Expression levels of transcription factor regulators of stomatal development (*SPCH*, *MUTE*, *FAMA*, *ICE1*) examined by qRT-PCR, 2h, 6h and 24h post-treatment with mock or 10μM DCMU. The expression of UBC21 served as internal control (n = 3 biologically independent samples). Difference between relative expression between mock and DCMU treated samples transformed in order to be represented as negative and positive values on a heat map. Numbers in bold indicate a significant difference between mock and DCMU treated at the relevant time point, using a Two-Tailed T-Tests (assuming unequal variance). Data used to construct the heat map can be found in Dataset S1.

Figure 1 is supported by Figure S1

**Figure 2: Cellular quantification of SPEECHLESS and MUTE following oxidation of the PQ pool.**

**A,** Fluorescence quantification of the cellular SPCH-GFP signal in cotyledons from *$SPCH_{pro}$:SPCH-GFP* seedlings following mock or 10 μM DCMU treatments. Seedlings were treated at 3 d.p.g and imaged 24h post-treatment. N ≥ 7 cotyledons imaged per treatment with ≥ 450 SPCH-GFP expressing cells in total counted per treatment. The 3D object counter plugin,[41] was used to segment fluorescent protein containing nuclei and quantify their fluorescent integrated density (mean intensity X volume), using consistent threshold intensities and minimum object sizes to ensure only nuclei were segmented. Box plot consists of 25$^{th}$ and 75$^{th}$ quartile with the line representing the median; whiskers are the minimum and maximum range. Two-Tailed T-Tests (assuming unequal variance) were performed between mock and DCMU treatments, P= 0.0036. See also Figures S2A.

**B,** Fluorescence quantification of the cellular MUTE-GFP signal in cotyledons from *$MUTE_{pro}$:MUTE-GFP* seedlings following mock or 10 μM DCMU treatments. Seedlings were treated at 3 d.p.g and imaged 24h post-treatment. N ≥ 5 cotyledons imaged per treatment with ≥ 48 MUTE-GFP expressing cells in total counted per treatment. The 3D object counter plugin,[41] was used to segment fluorescent protein containing nuclei and quantify their fluorescent integrated density (mean intensity X volume), using consistent threshold intensities and minimum object sizes to ensure only nuclei were segmented. Box plot consists of 25$^{th}$ and 75$^{th}$ quartile with the line representing the median; whiskers are the minimum and maximum range. Two-Tailed T-Tests (assuming unequal variance) were performed between mock and DCMU treatments, P= 0.0415. See also Figures S2A.

**C**, Stomatal Index of cotyledons 6 d.p.g DCMU for both Col-0 and *$SPCH_{pro}$:SPCH1-4A-YFP* seedlings following a single mock or 10 μM DCMU treatment at 3 d.p.g. Epidermal counts taken from at least 36 cotyledons from >18 independent plants. Box plot consists of 25$^{th}$ and 75$^{th}$ quartile with the line representing the median; whiskers are the minimum and maximum range. Two-Tailed T-Tests (assuming unequal variance) were performed on each genotype tested between mock and DCMU treatments (Col-0 P= 0.000356, SPCH1-4A P= 0.268).

**D,** Fluorescence quantification of the cellular SPCH-GFP and SPCH1-4A-YFP signal in cotyledons from *$SPCH_{pro}$:SPCH-GFP* and *$SPCH_{pro}$:SPCH1-4A-YFP* seedlings following mock or 10 μM DCMU treatments, respectively. Seedlings were treated at 3 d.p.g and imaged 24h post-treatment. N ≥ 10 cotyledons imaged per treatment with ≥ 236 and ≥ 759 for SPCH-GFP and

SPCH1-4A-YFP expressing cells in total counted per treatment respectively. The 3D object counter plugin, [41] was used to segment fluorescent protein containing nuclei and quantify their fluorescent integrated density (mean intensity X volume), using consistent threshold intensities and minimum object sizes to ensure only nuclei were segmented. Box plot consists of 25$^{th}$ and 75$^{th}$ quartile with the line representing the median; whiskers are the minimum and maximum range. A two-way ANOVA showed significant differences between treatments ($p<0.0001$), genotype ($p<0.0001$) and interaction ($p<0.0001$). Letters denote significance with a posthoc Tukey test. Alpha = 0.05. See also Figures S2B.

**E,** Representative confocal surface projections of *SPCH$_{pro}$:SPCH-GFP* and *SPCH$_{pro}$:SPCH1-4A-YFP* following mock or 10 μM DCMU treatments. GFP/YFP is the green channel and cells are counterstained with propidium iodide (grey). Chloroplast fluorescence is magenta. Scale bar = 20 μm.

**F,** Expression levels of regulators of stomatal development (*SPCH*, *MUTE*, *ICE1*, *EPF2*) examined by qRT-PCR, 6h post-treatment with mock or 10μM DCMU for both Col-0 and *SPCH$_{pro}$:SPCH1-4A-YFP* seedlings. The expression of *UBC21* served as internal control. The error bars indicate the SEM (n = 3 biologically independent samples). Two-Tailed T-Tests (assuming unequal variance) were performed on each time gene tested between mock and DCMU treatments of the respective genotype (p value * = < 0.05).

Figure 2 is supported by Figure S2

**Figure 3: Chloroplast signals act through MPK6 to inhibit stomatal development.**

**A,** Stomatal Index of cotyledons 6 d.p.g DCMU for both Col-0 and *STOM OE* seedlings following a single mock or 10 μM DCMU treatment at 3 d.p.g. Epidermal counts taken from at least 36 cotyledons from >18 independent plants. Box plot consists of 25$^{th}$ and 75$^{th}$ quartile with the line representing the median; whiskers are the minimum and maximum range. Two-Tailed T-Tests (assuming unequal variance) were performed on each genotype tested between mock and DCMU treatments. Col-0 P= 0.000002467, STOM OE P= 0.00275.

**B,** Expression levels of regulators of stomatal development (*SPCH*, *MUTE*, *EPF2*) examined by qRT-PCR, 6h post-treatment with mock or 10μM DCMU for Col-0 and *STOM OE*. The expression of *UBC21* served as internal control. The error bars indicate the SEM (n = 3 biologically independent samples). Two-Tailed T-Tests (assuming unequal variance) were

performed on each time gene tested between mock and DCMU treatments of the respective genotype (P values are indicated by * and **. * < 0.05; ** < 0.01).

**C,** Phosphorylation of Arabidopsis MPK6 and MPK3 after treatment with 10 μM DCMU. Analysis carried out with human phosphop44/42 antibodies (pERK1/2) on protein extracts obtained after 0, 5, 15, 30 and 60 min of treatment. MPK6phospho indicate phosphorylation. A loading control carried out with anti-MPK6 antibodies is shown in the lower panel. See also Figures S3E and S3F.

**D,** Stomatal Index of cotyledons 6 d.p.g DCMU for both Col-0 and *mpk6* seedlings following a single mock or 10 μM DCMU treatment at 3 d.p.g. Epidermal counts taken from at least 36 cotyledons from >18 independent plants. Box plot consists of 25$^{th}$ and 75$^{th}$ quartile with the line representing the median; whiskers are the minimum and maximum range. Two-Tailed T-Tests (assuming unequal variance) were performed on each genotype tested between mock and DCMU treatments. Col-0 P= 0.0132.

**E,** Expression levels of regulators of stomatal development (*SPCH*, *MUTE*, *ICE1*, *EPF2*) examined by qRT-PCR, 6h post-treatment with mock or 10μM DCMU for both Col-0 and *mpk6* seedlings. The expression of *UBC21* served as internal control. The error bars indicate the SEM (n = 3 biologically independent samples). Two-Tailed T-Tests (assuming unequal variance) were performed on each gene tested between mock and DCMU treatments of the respective genotype (p value ** = < 0.01).

**F,** Dual-luciferase assays showing relative luciferase activity in Arabidopsis protoplasts transiently transformed with *MUTEpro:LUC 35Spro:RENILLA* and either *35Spro:SPCH* or *35Spro:MUTE*. Relative luciferase activities were normalised to *Renilla* luciferase activities. The error bars indicate the SEM (n = 3 biologically independent samples). One-way ANOVA was performed to test statistical difference; letters denote significance with a posthoc Tukey test. Alpha = 0.05.

Figure 3 is supported by Figure S3

**Figure 4: HDG2 activity is required in this chloroplast signalling pathway.**

**A,** Expression levels of regulators of stomatal development (*SPCH*, *MUTE*, *EPF2*) examined by qRT-PCR, 6h post-treatment with mock or 10μM DCMU for Col-0 and *hdg2*. The expression of *UBC21* served as internal control. The error bars indicate the SEM (n = 3 biologically independent samples). Two-Tailed T-Tests (assuming unequal variance) were performed on

each time gene tested between mock and DCMU treatments of the respective genotype (P * = < 0.05 and ** = < 0.01).

**B,** Stomatal Index of cotyledons 6 d.p.g DCMU for both Col-0 and *hdg2* seedlings following a single mock or 10 µM DCMU treatment at 3 d.p.g. Epidermal counts taken from at least 36 cotyledons from >18 independent plants. Box plot consists of 25$^{th}$ and 75$^{th}$ quartile with the line representing the median; whiskers are the minimum and maximum range. Two-Tailed T-Tests (assuming unequal variance) were performed on each genotype tested between mock and DCMU treatments. Col-0 P= 0.00227

**C,** Dual-luciferase assays showing relative luciferase activity in Arabidopsis protoplasts transiently transformed with *SPCHproLUC 35SproRENILLA* and either *35Spro:HDG2*, *35Spro:MPK6* or both. Relative luciferase activities were normalised to *Renilla* luciferase activities. The error bars indicate the SEM (n = 3 biologically independent samples). One-way ANOVA was performed to test statistical difference; letters denote significance with a posthoc Tukey test. Alpha = 0.05.

**D,** Dual-luciferase assays showing relative luciferase activity in Arabidopsis protoplasts transiently transformed with *MUTEproLUC 35SproRENILLA* and either *35Spro:HDG2*, *35Spro:MPK6* or both. Relative luciferase activities were normalised to renilla luciferase activities. The error bars indicate the SEM (n = 3 biologically independent samples). One-way ANOVA was performed to test statistical difference; letters denote significance with a posthoc Tukey test. Alpha = 0.05.

**E**, HDG2 interacts with MPK6. *In vitro* pull downs were performed with recombinant proteins isolated from *E. coli.* Proteins were incubated in the presence of ATP before affinity purification with amylose beads. Proteins were eluted using maltose and analysed using western blot using HIS and MBP antibodies. See also Figures S4G.

**F**, MPK6 phosphorylates HDG2. *In vitro* kinases assays were performed with recombinant proteins isolated from *E. coli.* Proteins were incubated (5:1 molecular ratio of MPK6/MKK5-CA:HDG2) in the presence of ATP before [$\gamma$-$^{32}$P] ATP was added for a further incubation. Samples were run on SDS-PAGE before detection with a phosphorscreen and phosphorimager. Coomassie gel and uncropped phosphoimage, see Figures S4G.

Figure 4 is supported by Figure S4

## STAR METHODS

### Resource Availability

### Lead Contact

Further information and requests for resources and reagents should be directed to and will be fulfilled by the Lead Contact, Stuart A. Casson (s.casson@sheffield.ac.uk).

### Materials availability

All unique/stable reagents generated in this study are available from the Lead Contact without restriction.

### Data and code availability

- Original western blot images are available in Figures S3 and S4. Microscopy data reported in this paper will be shared by the lead contact upon request.
- This paper does not report original code.
- Any additional information required to reanalyze the data reported in this paper is available from the lead contact upon request.

## EXPERIMENTAL MODEL AND SUBJECT DETAILS

The Arabidopsis ecotype Columbia-0 (Col) was used as the wild-type control in all experiments except in the far-red *phyQ*[26] experiments which is based in the *Ler* background. The following transgenic lines and mutants employed in the study were reported previously: *SPCH*$_{pro}$*:SPCH-GFP;*[3] *SPCH*$_{pro}$*:SPCH1-4A-YFP;*[4] *STOM OE;*[28] *mpk6* (salk_062471);[42] *atml1* (SALK_128172);[43] *hdg2* (salk_138646C);[43] *cas-1* (salk_070416);[33] *csk* (salk_125411);[34]; *pif4-101*;[44] *stn7*;[22] *tap38.*[23]

Seedlings for stomatal counts, cotyledon measurements, and qRT-PCR analysis were grown on Levingtons F2+sand compost in environmental control chambers (Conviron BDR16) at an irradiance of ~250 µmol $m^{-2}$ $s^{-1}$, a constant temperature (22°C) and a 12h photoperiod. For treatments with DCMU (#D2425-100g; Sigma Aldrich, Poole, UK), seedlings were sprayed at zeitgeber (ZT) 2 with 10µM DCMU, 0.01% Silwet L-77 (#VIS-30; Lehle Seeds, Round Rock, USA) or mock sprayed with 0.01% Silwet L-77. Norflurazon (5µM; #34364-100MG; Sigma Aldrich, Poole, UK) treatments were performed in the same manner.

For low light to high light (LL to HL) experiments, plants were grown for 9 d.p.g at ~50 µmol $m^{-2}$ $s^{-1}$ then transferred (ZT2) to ~250 µmol $m^{-2}$ $s^{-1}$ for 6h (ZT8). For high light to low light (HL to LL) plants were grown for 7 d.p.g at ~250 µmol $m^{-2}$ $s^{-1}$ then transferred to ~50 µmol $m^{-2}$ $s^{-1}$ for 6h. For far-red experiments plants grown for 7 d.p.g. in ~250 µmol $m^{-2}$ $s^{-1}$ (WL) before being transferred (ZT2) to ~50 µmol $m^{-2}$ $s^{-1}$ far-red light for 6h (ZT8). *β*-Estradiol (Sigma Aldrich, Poole, UK) induction of *iSPCH* plants was performed by treating 7 d.p.g. seedlings (ZT2) with EtOH, 0.01% Silwet L-77 (mock) or 10µm *β*-Estradiol, 0.01% Silwet L-77 for 6h (ZT8) prior to harvest.

For confocal quantification $SPCH_{pro}$*:SPCH-GFP*, $SPCH_{pro}$*:SPCH1-4A-YFP* or $MUTE_{pro}$*:MUTE-GFP* seeds were surface sterilised for 30s in 70% ethanol and 10 minutes in 10 % commercial bleach, and washed three times in sterile $H_2O$ before being sown on sterile ½ MS containing 8 g/l agar. Seeds were stratified for 3 days at 4 °C and then grown for three days post-germination. Seedlings were sprayed (ZT2) with either 10 µM DCMU, 0.01% Silwet L-77 or mock sprayed with 0.01% Silwet L-77 and grown for a further 24 hours before imaging.

For DBMIB (#271993, Sigma) stomatal counts, Col-0 seeds were surface sterilised for 30s in 70% ethanol and 10 minutes in 10 % commercial bleach, then sown on sterile ½ MS containing 8 g/l agar, as well as ethanol (mock) or 40 µM DBMIB. Seeds were stratified for 3 days at 4 °C and then grown for six days post-germination. Growth of Col-0 seedlings for RT-PCR with DBMIB was performed as follows, seeds were surface sterilised for 30s in 70% ethanol and 10 minutes in 10 % commercial bleach, ~ 25 seeds were aliquoted into 6 well tissue culture plates containing 2 mL of ½ MS media and left to stratify for 3 days. After stratification, plates were transferred to environmental control chambers (Conviron BDR16) at an irradiance of ~50 µmol $m^{-2}$ $s^{-1}$ on a shaking platform (25 rpm) for 6 d.p.g. Mock (ethanol) or 40 µM DBMIB were added (ZT2) and treatment left for 6 hours (ZT8), after which samples were snap frozen in liquid nitrogen for processing at a later date.[17]

## METHOD DETAILS

*Stomatal counts*

Impressions of the abaxial surface of cotyledons were made using dental resin (Impress Plus Wash Light Body, Perfection Plus Ltd, Totton, UK). Clear nail varnish was applied to the set impression after removal from the cotyledon, and Z-stack images captured at 20X on a Brunel

n300-M microscope equipped with a Prior ES10ZE Focus Controller and Moticam 5 camera. 36 cotyledons for each genotype (area 0.24 $mm^{-2}$) were examined per experiment and statistical analysis performed using GraphPad Prism.

*Cotyledon Measurements*

Lecia S9i stereo microscope with an integrated camera was used to capture images of 6 d.p.g. DCMU treated seedlings. ImageJ software was used to measure cotyledon area. Experiments were performed in triplicate and statistical analysis performed using GraphPad Prism (N=30).

*RNA extractions and quantitative RT-PCR*

Seedlings of all lines tested were grown to 7 d.p.g. and treated (ZT2) as previously described. 100mg of seedling tissue (approximately 20 seedlings) was collected in Eppendorf 2 ml safe lock tubes (#0030120094; Eppendorf, Stevenage, UK) containing a 5 mm steel ball bearing and flash frozen in liquid nitrogen. Plant tissue was disrupted in a TissueLyser II (Qiagen; Manchester, UK) and RNA extracted using a Quick-RNA™ MiniPrep kit (#R1055a; Zymo Research, Irvine, USA) according to the manufacturer's instructions including an on column DNase step. RNA was quantified using UV spectroscopy on a BioDrop™ (BioDrop™ DUO, Biochrom Ltd, UK). 2µg of total RNA was reverse transcribed using the High-Capacity cDNA Reverse Transcription kit with random hexamers (#4368814; Applied Biosystems, Foster City, USA). cDNA was diluted 20X in $ddH_2O$ prior to qPCR. SYBR® Green JumpStart™ Taq ReadyMix (#S5193; Sigma-Aldrich, Poole, UK) was used for qPCR (15 µL reaction volume [7.5µL x2 Taq Ready Mix, 3.75µL cDNA, 2.1µL $MgCl_2$ 25mM, 0.9µL nuclease-free water, 0.75µL 7.5µM forward and reverse primer mix]) and was performed using a CFX Connect Real-Time PCR Detection System (Bio-Rad, Watford, UK) with 40 cycles of 95°C-10s, 57°C-10s 72°C-15s and a final dissociation curve. Relative expression of target genes in the different samples was calculated from *UBC21* or *UBQ10* [45] normalized target signals using the $2^{-\Delta\Delta CT}$ method. [46] Untransformed $2^{-\Delta\Delta CT}$ data used in Figure 1H and Figure S1I can be found in Data S1.

*Confocal microscopy and image quantification*

Seedlings were counterstained for 3 minutes with 20mg/l propidium iodide (PI; #P4170; Sigma-Aldrich, Poole, UK), transferred to $ddH_2O$ for 1 minute, and then mounted in $ddH_2O$ without the hypocotyl and root. Seedlings were imaged with an Olympus FV1000 confocal laser scanning microscope with a 40X oil lens, producing Z-stacks through the abaxial epidermis. GFP was excited with the 488 nm laser line. YFP was excited with the 515 nm laser line. PI and

chloroplasts were excited with the 543 nm or 559 nm laser line. Microscope settings were not changed between cotyledons of the same line to ensure cross comparability.

The FIJI distribution of ImageJ2 was used to analyse images.[47] The Bioformats plugin was used to import images.[48] The Spectral Unmixing plugin (Joachim Walter, v 1.3 https://imagej.nih.gov/ij/plugins/spectral-unmixing.html) was used to remove any autofluorescence from the fluorescent protein channel. Unmixing matrices were calculated from regions containing only the fluorescent protein, chloroplast or background and post-processing background florescence was measured to ensure consistency between stacks. A median filter was performed to remove noise from images (sigma = 2). The 3D object counter plugin,[41] was used to segment fluorescent protein containing nuclei and quantify their fluorescent integrated density (mean intensity X volume), using consistent threshold intensities and minimum object sizes to ensure only nuclei were segmented. Over and under segmentation was checked visually and segmentation mistakes were removed from the dataset. To quantify the proportion of *SPCH-GFP* and *MUTE-GFP* containing cells, all cells were counted manually in FIJI, on raw images or EZ Peeler [49] surface projections (Data S1).

*Image rendering*

Because a leaf epidermis is not flat, projecting a series of confocal Z planes into a 2D image is difficult without including cells from underlying mesophyll, obscuring the tissue of interest with strong autofluorescence. A plugin (EZ-Peeler v 0.16) [49] was previously written for ImageJ to segment the contour of the epidermis and extract the data from user defined depth below this contoured surface. Confocal images are Z sum projections of these segmented images (Surface projections). Source code is available at https://github.com/JimageJ/EZ-Peeler .

*Chlorophyll Fluorescence measurements*

Chlorophyll fluorescence measurements were performed on 3 d.p.g. or 7 d.p.g. plants to match the ages used in stomatal counts and gene expression analysis, respectively. A WALZ Imaging-PAM MAXI fluorimeter (Walz, Effeltrich, Germany), was used for all imaging.

DCMU timecourse

Plants were sprayed with either 10 µM DCMU, 0.01 % Silwet L-77 or mock sprayed with 0.01 % Silwet L-77. After 0, 2, 6, 24, 48 and 72 hours, plants were removed from the growth chamber dark adapted for 10 minutes and then after initial Fv/Fm measurement, a 230 µmol $m^{-2}$ $s^{-1}$ actinic light was used to give conditions close to growth conditions with a 1500 µmol $m^{-2}$ $s^{-1}$

saturating pulse every 20s for 5 minutes. A minimum of three independent pots of seedlings were used.

DBMIB measurements

For DBMIB (#271993, Sigma) stomatal counts, Col-0 seeds were surface sterilised for 30s in 70% ethanol and 10 minutes in 10 % commercial bleach, then sown on sterile ½ MS containing 8 g/l agar, as well as ethanol (mock) or 40 µM DBMIB. Seeds were stratified for 3 days at 4 °C and then grown for six days post-germination. Plates were removed from the growth chamber dark adapted for 10 minutes and then after initial Fv/Fm measurement, a 230 µmol $m^{-2}$ $s^{-1}$ actinic light was used with a 1500 µmol $m^{-2}$ $s^{-1}$ saturating pulse every 20s for 5 minutes.

Col-0 light curve

Plants were grown for three weeks, dark adapted for 30 minutes and an Fv/Fm measurement was taken. Light curves were performed with actinic light intensities of 55, 90, 130, 230, 500, 1030 µmol $m^{-2}$ $s^{-1}$ saturating pulses of 1500 µmol $m^{-2}$ $s^{-1}$ every minute for 12 minutes. Because the plants were not moved between measurements, three whole leaf ROIs were drawn manually on two plants.

*Molecular cloning and transformation*

To construct the *MUTE$_{pro}$:MUTE-GFP* construct, the GFP coding sequence from *pGKGW-G* [50] was amplified using the primers GFP221Pac1for and GFP221Pvu1rev (see Table S1 for all primer sequences) using Q5® High-Fidelity DNA Polymerase (New England Biolabs). The PCR fragment was digested with PacI and PvuI and cloned into PacI digested *pMDC221*[51] to create *pMDC221-GFP*. A 3.1kb genomic fragment of *MUTE* containing 1.5kb of 5' sequence was amplified from Col-0 genomic DNA using Q5® High-Fidelity DNA Polymerase (New England Biolabs) and the primers MUTE-Apa1For and MUTE-Pvu1Rev. This fragment was cloned in frame with the coding sequence of GFP into ApaI-PacI digested binary vector *pMDC221-GFP.*

To construct the inducible *iSPCH lines* (*35SproXVE; LexA::SPCH*), *SPCH* cDNA was cloned into MDC150 35SproXVE; LexA-GFP.[51] These constructs are based on those described in. [51] The vector pMDC150 was modified so that all elements of the system are found on one vector (XVE transcriptional activator and LexA promoter). The LexA promoter was amplified from pMDC221[51] using using Q5® High-Fidelity DNA Polymerase (New England Biolabs) and the primers LexA150proFor and LexA150proRev. GFP coding sequence and the CaMV35S terminator sequence were amplified from pGKGWG[50] using using Q5® High-Fidelity DNA

Polymerase (New England Biolabs) and the primers GFP150ageIFor and GFP150terRev. The fragments were digested with AgeI, ligated and then used as a PCR template using the primers LexA150proFor and GFP150terRev. This fragment was digested with KpnI and ligated into PmeI-KpnI digested pMDC150 to generate pMDC150-LexA-GFP. The CaMV35S promoter was then amplified from pMDC32[52, 53] using the primers 35S(mdc32)AscFor and 35S(mdc32)PacIRev, digested with AscI and PacI and ligated into AscI-PacI digested pMDC150-LexA-GFP to create pMDC150 35SproXVE; LexA-GFP. SPCH was amplified from Col-0 cDNA using using Q5® High-Fidelity DNA Polymerase (New England Biolabs) and the primers SPCHbsiwFor/SPCHxho1Rev2. cDNAs were digested with BsiWI/XhoI and ligated into MDC150 based vectors cut with BsiWi/XhoI.

Both newly generated constructs were verified by Sanger sequencing before being transformed into Col-0 plants using the floral-dip method.[54] Transformants (~15) were screened for on ½ MS containing 8 g/l agar containing 50µg/mL Gibco™ Kanamycin Sulfate (Fisher Scientific, UK) or 25 µg/mL Hygromycin B (cambridge bioscience, UK). The Mendelian inheritance of the selection marker was used to identify homozygous lines.

*Protoplast Isolation and Transfection*

Protoplasts were isolated using the 'Tape-*Arabidopsis*-Sandwich' method.[55] In brief, mature leaves (7-10 fully expanded leaves) of 4-5 week old *Arabidopsis* (Col-0) grown in 250 µmol $m^{-2} \cdot s^{-1}$ of light were collected and had a strip of autoclave affixed to the adaxial surface. The excess tape was cut from around the leaf, and then another strip of autoclave tape was affixed to the abaxial surface. The piece of tape affixed to the abaxial surface was then carefully peeled away exposing the mesophyll layers. Following the removal of the abaxial epidermis, leaves were incubated in a petri dish containing 10 ml of enzyme solution [1% cellulase 'Onozuka' R10 (Duchefa Biochemie, Netherlands), 0.25% macerozyme 'Onozuka' R10 (Duchefa Biochemie, Netherlands), 0.4 M mannitol, 10 mM $CaCl_2$, 20 mM KCl, 0.1% BSA and 20 mM MES, pH 5.7] for 1 hour on a shaking platform (50rpm). Following the incubation the enzyme solution now containing the protoplasts was centrifuged at 100 × *g* for 3 minutes in a centrifuge (3K15, Sigma), and then washed twice with 25 mL of pre-chilled W5 solution (154 mM NaCl, 125 mM $CaCl_2$, 5 mM KCl, 5 mM glucose, and 2 mM MES, pH 5.7). The protoplasts were incubated on ice for 30 minutes and during the incubation, the protoplasts were counted using a hemocytometer visualised under a light microscope. The protoplasts were centrifuged at 100 x g for three minutes and resuspended in MMg solution (0.4 M mannitol, 15 mM MgCl2, and 4 mM MES, pH 5.7) to a final density of $5x10^5$ cells/ml. 1 x $10^5$ protoplasts suspended in MMg were

mixed with 10-40µg of plasmid DNA at room temperature, before being slowly mixed with a freshly-prepared solution of 40% PEG 4000 (40% PEG MW 4000, 0.1 M CaCl2 and 0.2 M mannitol) and left to incubate for 10 minutes at room temperature. Following incubation, the protoplast PEG mixture was slowly washed with 3ml of W5 solution and centrifuged for 1 minute at 100 x g. The W5 wash of the protoplasts was repeated twice, following the final wash the protoplasts were resuspended in 1 ml of W5 and incubated for 16-24 hours in the original growth conditions of the mature plants used for protoplasting.

*Dual Luciferase Assays*

To construct the *SPCHproLUC* and *MUTEproLUC* constructs, the *SPCH* (2kb) and *MUTE* (3kb) promoter sequences were amplified from genomic Col-0 DNA using the primers SPCHproFor-KpnI, SPCHproRev-NcoI, MUTEproFor-KpnI and MUTEproRev-NcoI respectively, using Q5® High-Fidelity DNA Polymerase (New England Biolabs). The SPCHpro and MUTEpro PCR fragments were digested with KpnI and NcoI and ligated into KpnI and NcoI digested pGreen800-Luc[56] (kindly provided by Roger Hellens) to create *SPCHproLUC* and *MUTEproLUC*. To construct *SPCH*, *MUTE* and *HDG2 pDH51-YFPc*,[50] as well as *MPK6 pDH51-YFPn*, full length CDS fragments were amplified (See supplemental table for primers) from cDNA using Q5® High-Fidelity DNA. *SPCH* and *MUTE* fragments were digested with BamHI and XhoI, then ligated into BamHI and XhoI cut *pDH51-YFPc* (*SPCH*, *MUTE*). *HDG2* fragments were digested with BclI and XhoI, then ligated into BamHI and XhoI cut *pDH51-YFPc. MPK6* PCR product and *pDH51-YPFn* were digested BamHI and SalI and ligated together. All plasmids were checked by sequencing.

Protoplasts were transfected with 10 µg of each individual construct used in the dual luciferase assay (typically 20-30 µg). Control protoplasts were transfected with an appropriate amount of water instead of plasmid DNA. Following a 16-24 hour incubation, protoplasts were harvested by spinning at 14,000 x g for 30 seconds. Dual luciferase assays were carried out using the Dual-Luciferase® Reporter Assay System (Promega), according to manufactures instructions. In Brief, the pellet of protoplasts were resuspended in 150 µL of 1 x passive lysis buffer and left to incubate for 15 minutes at room temperature. Approximately 6.6 x $10^4$ cells were used per replicate. After incubation, 20 µL of lysed protoplasts were added to 100 µL of LARII, briefly vortexed and luminescence measured immediately (Sirius Luminometer, Berthold Detection Systems). Luciferase luminescence was stopped and *Renilla* luminescence measured by the addition of 100 µL of Stop & Glo® Buffer. Luminescence was measured in technical triplicates for all combinations of transfected plasmids.

*MPK6 immunoblots*

For analysis of MPK6 activation, seedlings were grown on ½ strength Murashige and Skoog (MS) agar media (0.8%) for 8 days post germination. 24 hours prior to treatment, seedlings were transferred to 20 mL of ½ strength MS in a petri dish. Two hours post-dawn DCMU was added to the seedlings in the petri dish to a concentration of 10 µM or the equivalent amount of EtOH for control samples. ~100 mg of tissue was collected and immediately frozen in liquid nitrogen at 0, 15, 30, and 60 minutes post-treatment. Frozen samples were ground with a ball bearing in a TissueLyser II (Qiagen; Manchester, UK) and protein extractions performed as detailed.[57, 58] Ground samples were weighed out and had a 6x Protein extraction/loading buffer (0.35 m Tris-HCl pH 6.8; 30% [v/v] glycerol; 10% [v/v] SDS; 0.6 m dithiothreitol; and 0.012% [w/v] bromophenol blue) added to it at a 1mg of tissue to a 1 µL of buffer ratio. The tissue/buffer mixture was vortexed vigorously then boiled at 95˚C for 10 minutes. After cooling for 3 minutes, samples were centrifuged at 11,000 x g for 5 minutes to precipitate debris. 15 µL of each sample was loaded into a 12% SDS-PAGE gel. Gels were equilibrated in transfer buffer prior to semidry transfer onto PVDF membranes, and blocked in 5% milk/1xTBS-T overnight at 4˚C.

Phosphorylated MPK3/6 was detected using a phospho-specific antibody (1:2000, Phospho-p44/42 MAPK (Thr202/Tyr204) Antibody; #9101; Cell Signaling Technology, Danvers, USA) and a secondary Goat Anti-Rabbit HRP antibody (1:5000, #ab6721, Abcam, Cambridge, UK). Chemiluminescent western blot detection was performed using Clarity Western ECL Substrate (Bio-rad, Watford, UK) and imaged using a ChemiDoc™ XRS+ System (Bio-rad). Following detection of the phosphorylated MPK3/6, blots were stripped using a mild stripping buffer (200mM glycine, 0.001% SDS w/v, 0.01% Tween-20) for 2x10 minutes incubations. After the incubations in the stripping buffer, membranes were washed with 1xPBS and 1xTBS-T twice respectively. Membranes were blocked once more in 5% milk/1xTBS-T overnight at 4˚C. MPK6 for loading control was detected using an anti-MPK6 antibody (1:10,000, #ab50186; Abcam, Cambridge, UK) and a donkey anti-Goat HRP antibody (1:20,000, #sc-2020; Santa Cruz Biotechnology, Dallas, USA).

*Yeast two-hybrid*

Plasmid construction

HDG2 and MPK6 CDS were each cloned into pADC and pBDC vectors respectively by homologous recombination. Both vectors are derived from pOBD2 with pBDC containing the Gal4 DNA Binding Domain and pADC containing the Gal4 Activation Domain.[59] HDG2 and

MPK6 CDS were amplified from cDNA using Q5® High-Fidelity DNA Polymerase (New England Biolabs) and the primers ADC-HDG2-For and ADC-HDG2-Rev; BDC-MPK6-For and BDC-MPK6-Rev. pADC and pBDC plasmids were cut with *NruI* and co-transformed with the CDS into S. cerevisiae BJ1991 (trp- leu-) strain. High efficiency yeast transformation was done according to the lithium acetate protocol.[60] Exponential phase YPD-grown yeast cells were spun down and washed with water, then treated with 1ml freshly made 1x TE/LiAc (10 mM Tris HCl (pH 8.0), 1 mM EDTA, 0.1 M Lithium acetate). Cells were pelleted and resuspended in 50µl of 1xTE/LiAc and mixed with 500ng digested vector, 500ng amplified insert, 10µg salmon sperm DNA and 300µl 40% PEG 3350/1x TE/LiAc solution. Reactions were incubated for 30 min at room temperature followed by 30 minutes at 30°C, then heat shocked for 15 min at 42°C. Cells were pelleted and resuspended in 50µl TE and plated on corresponding trp- or leu- selective media plates and grown for 3 days at 30°C. To extract successfully recombined constructs, a colony was grown up overnight in selective liquid medium and cells were spun down. The pellet was washed in water, then mixed with 400µl TENTS (20mM Tris-HCl pH 8.0, 1mM EDTA, 100mM NaCl, 2% Triton-x100), 200µl glass beads and 200µl phenol:chloroform. Cells were then broken with a cell homogeniser and spun down to eliminate cell debris. The supernatant was mixed with 200µl TENTS, centrifuged and the supernatant isolated. 200µl of phenol:chloroform was then added, centrifuged and the supernatant isolated. Plasmid DNA was precipitated by centrifugation following the addition of 1/10 volume of 3M NaAc pH 5.2 and 2.5 volume of ice cold 100% ethanol, followed by a 70% ethanol wash. The pellet was dissolved in 200µl TE with 2µl of RNAse and incubated at RT for 10 min. The DNA was then precipitated a further time by centrifugation following the addition of 1/10 volume of 3M NaAc pH 5.2 and 2.5 volume of ice cold 100% ethanol, followed by a 70% ethanol wash. Purified plasmid DNA was transformed into E. coli DH5α cells following the standard protocol. *E. coli* colonies were screened by PCR and plasmids isolated to obtain ADC-HDG2 and BDC-MPK6.

Transformation

The AD and BD plasmids were transformed using 50µl one step transformation buffer (0.2M lithium acetate pH 5.0, 40% Polyethylene glycol 3350, 100mM Dithiothreitol) and 5µl salmon sperm DNA into the PJ69-4A yeast strain (*MATα, trp1-901, leu2-3,112, ura3-52, his3-200, gal4Δ, gal80Δ, LYS2::GAL1-HIS3, GAL2-ADE2, met2::GAL7-lacZ*).[61] Transformants were selected on SDC-leu-trp plates and grown at 30°C for two days. Transformants were replica plated onto SDC-leu-trp and SDC-leu-trp-ade plates to check all colonies. To assess growth,

individual clones were spotted in 10-fold serial dilutions onto SDC-Trp-Leu or SDC-Leu-Trp-Ade plates and grown at 30°C for 2 days.

*Recombinant protein expression and purification*

Plasmid construction

HDG2 (TAIR AT1G05230), MPK6 (TAIR AT2G43790) and MKK5 (TAIR AT3G21220) CDS were amplified without stop codons using Q5® High-Fidelity DNA Polymerase (New England Biolabs) and the specific primers (see Supplemental Table 1 for primer sequences) from an *A. thaliana* cDNA library. Amplified HDG2 cDNA was cloned into pET28a containing HISx6-MBP using Gibson assembly (New England Biolabs). Following amplification MPK6 and MKK5 CDS were cloned into pET2817 [62] via gibson assembly and restriction digestion respectively. MKK5 clones underwent site direct mutagenesis to recreate a consistutively active MKK5 (MKK5-CA). All clones where introduced to BL21-CodonPlus(DE3)-RIL (Agilent Technologies).

*Protein expression and purification*.

BL21 cells were grown to an $OD_{600}$ of 0.5 at 37°C before being incubated at 18°C for 30 minutes. BL21 cells were induced using 1 mM IPTG and grown for 16 hours at 18°C. Cells were pelleted before being resuspended in 0.5M NaCl 50mM Tris pH 8.0 and sonicated (3 X 20sec at 16 micron amplitude using a Soniprep150). Sonicated samples were pelleted at 72,000x g for 10 minutes to obtain cell free extract. Hisx6-MPK6 was purified using a 5mL His-Trap HP column on AKTA purifier system and eluted using a gradient of 0 to 350 imidazole. Fractions containing Hisx6-MPK6 were further purified by gel filtration on a 1.6x60cm Hi Load Superdex200 column on AKTA purifier in resuspension buffer. Hisx6-MPK6 were then concentrated using a Vivaspin 20, 10,000 MWCO (Sartorius Group, Germany). StrepII-MKK5-CA was purified on a 1mL Strep-Trap HP column, eluted using 2.5mM desthiobiotin, Tris-HCl 50mM pH 7.5, 0.15M NaCl, 1mM EDTA, before being concentrated with a Vivaspin 20, 10,000 MWCO. Hisx6-MBP-HDG2 was purified using an 8ml amylose column, washed with 25ml of resuspension buffer and eluted 10mM maltose in resuspension buffer. Gel filtration was performed on Hisx6-MBP-HDG2 containing fractions using a Superdex200 Increase column. The fraction with the purest (90%) Hisx6-MBP-HDG2 was used for downstream experiments.

*In Vitro* pull down assays

Pull down assays using purified recombinant protein were performed with 3 µg HISx6-MBP-HDG2 as bait, 5 µg MPK6 as the prey, and 5 µg Mkk5-CA as an activator in 1x kinase buffer (50 mM HEPES (pH 7.5), 75 mM NaCl, 1 mM MgCl2, 1mM ATP). MBP replaced HISx6-MBP-HDG2 as a control and was used at the same molecular ratio. Samples were incubated at 30°C for 30 minutes before mixed end over end with 50 µL of Amylose Magnetic Beads for 1 hour. Beads were washed three times in kinase buffer without ATP before incubation with 10mM maltose for 1 hour. Eluted samples were used in western blots to detect interactions.

Western blotting

Detection of pull downed proteins was preformed using western blotting. 25 µL of each pull down sample (boiled with 5 µL of 6x SDS loading buffer) was loaded into a 10% SDS-PAGE gel. Gels were equilibrated in transfer buffer prior to semidry transfer onto PVDF membranes, and blocked in 5% milk/1xTBS-T overnight at 4˚C. MBP tagged and HIS tagged proteins were detected using specific antibodies ( anti-MBP primary antibody [1:2,000 #GTX124267; Genetex, Taiwan ] and anti-HIS primary antibody [1:2,000 #652502; Biolegend, USA] respectively) and secondary antibodies (Goat Anti-Rabbit HRP antibody [1:10,000, #ab6721, Abcam, Cambridge, UK] and a Goat Anti-Mouse HRP antibody[1:10,000 # sc-2005, Santa Cruz Biotechnologies, USA]). Chemiluminescent western blot detection was performed using Clarity Western ECL Substrate (Bio-rad, Watford, UK) and imaged using a ChemiDoc™ XRS+ System (Bio-rad).

*In Vitro* kinase assay

Recombinant proteins used at a molecular ratio of 5:1 kinases (MPK6 and MKK5-CA) to substrate (HIS-MBP-HDG2 or MBP). MPK6 and MKK5-CA were mixed in 1x kinase buffer (50 mM HEPES (pH 7.5), 75 mM NaCl, 1 mM MgCl2, 1mM ATP) for 30 minutes at 30°C. [γ-32P] ATP (3 µCi) and substrate (HIS-MBP-HDG2 or MBP) were spiked into the mixture and incubated for an additional 30 minutes at 30°C. Samples were boiled in x1 SDS loading buffer for 5 minutes before being loaded into 4-12% Bis-Tris gradient gels. Proteins were visualised by coomassie staining before $^{32}P$ signal was detected and imaged using the being imagined with a phosphoimager Typhoon FLA 7000, imager (GE Healthcare; Scan settings-650nm laser, IP filter, and 50uM pixel resolution).

*Electrophoresis mobility shift assay (EMSA)*

DNA probes for EMSAs were made from a 55bp oligonucleotide fragment of the *SPCH* promoter (for sequences see Table S1) that were annealed to the reverse compliment by heating at 95°C for 5 minutes in annealing buffer (10 mM Tris-HCl pH 8.0, 1 mM EDTA, 50 mM NaCl) before slowly cooling to 25°C over the course of an hour. The fluorescent oligonucleotide were synthesised with a 5' end label of HEX$^{tm}$ (Sigma-Aldrich, UK), recombinant proteins used at a molecular ratio from 3:1 to 24:1 (HIS-MBP-HDG2 or MBP [24:1, NKMAX, KR]) to DNA probe. Unlabelled probe was added at 25:1 and 50:1 molecular ratio to the labelled probe in competition assays. Protein and DNA probes were mixed in buffer (10 mM Tris-HCl pH 8.0, 1 mM EDTA, 50 mM NaCl) and left to incubate for 30 minutes at 4°C. Samples and ladder (GeneRuler DNA Ladder, Thermo Scientific) were mixed with loading dye and run on a 1% agarose gel in 1xTBE at 4°C. Gel was imaged with a Typhoon FLA 7000, imager (GE Healthcare; Scan settings 530nm laser, 580nm filter, and 25uM pixel resolution) to detect HEX-labelled probe.

## QUANTIFICATION AND STATISTICAL ANALYSIS

Initial data was stored and organised in Microsoft Excel, and then processed in GraphPad Prism v 9. Two-Tailed T-Tests (assuming unequal variance) were performed in Excel, all other statistics were performed in GraphPad.

## SUPPLEMENTAL INFORMATION

### Data S1. Complete data sets related to Figures 1, 2, and S1.

Untransformed qRT-PCR data used to generate Heatmaps in Figure 1H and Figure S1I. Data and statistical output of two-sided chi square test for SPCH-GFP and MUTE-GFP expressing cells. Related to STAR Methods.

## REFERENCES


1. Assmann, S.M., and Jegla, T. (2016). Guard cell sensory systems: recent insights on stomatal responses to light, abscisic acid, and CO2. Curr Opin Plant Biol *33*, 157-167.

2. Kanaoka, M.M., Pillitteri, L.J., Fujii, H., Yoshida, Y., Bogenschutz, N.L., Takabayashi, J., Zhu, J.-K., and Torii, K.U. (2008). SCREAM/ICE1 and SCREAM2 Specify Three Cell-State Transitional Steps Leading to Arabidopsis Stomatal Differentiation. The Plant Cell *20*, 1775-1785.

3. MacAlister, C.A., Ohashi-Ito, K., and Bergmann, D.C. (2007). Transcription factor control of asymmetric cell divisions that establish the stomatal lineage. Nature *445*, 537-540.

4. Lampard, G.R., MacAlister, C.A., and Bergmann, D.C. (2008). Stomatal Initiation Is Controlled by MAPK-Mediated Regulation of the bHLH SPEECHLESS. Science *322*, 1113.

5. Wang, H., Ngwenyama, N., Liu, Y., Walker, J.C., and Zhang, S. (2007). Stomatal Development and Patterning Are Regulated by Environmentally Responsive Mitogen-Activated Protein Kinases in Arabidopsis. The Plant Cell *19*, 63.

6. Putarjunan, A., Ruble, J., Srivastava, A., Zhao, C., Rychel, A.L., Hofstetter, A.K., Tang, X., Zhu, J.K., Tama, F., Zheng, N., et al. (2019). Bipartite anchoring of SCREAM enforces stomatal initiation by coupling MAP kinases to SPEECHLESS. Nat Plants *5*, 742-754.

7. Hara, K., Kajita, R., Torii, K.U., Bergmann, D.C., and Kakimoto, T. (2007). The secretory peptide gene EPF1 enforces the stomatal one-cell-spacing rule. Genes & Development *21*, 1720-1725.

8. Hara, K., Yokoo, T., Kajita, R., Onishi, T., Yahata, S., Peterson, K.M., Torii, K.U., and Kakimoto, T. (2009). Epidermal Cell Density is Autoregulated via a Secretory Peptide, EPIDERMAL PATTERNING FACTOR 2 in Arabidopsis Leaves. Plant and Cell Physiology *50*, 1019-1031.

9. Sugano, S.S., Shimada, T., Imai, Y., Okawa, K., Tamai, A., Mori, M., and Hara-Nishimura, I. (2010). Stomagen positively regulates stomatal density in Arabidopsis. Nature *463*, 241-244.

10. Pillitteri, L.J., Sloan, D.B., Bogenschutz, N.L., and Torii, K.U. (2007). Termination of asymmetric cell division and differentiation of stomata. Nature *445*, 501-505.

11. Peterson, K.M., Shyu, C., Burr, C.A., Horst, R.J., Kanaoka, M.M., Omae, M., Sato, Y., and Torii, K.U. (2013). Arabidopsis homeodomain-leucine zipper IV proteins promote stomatal development and ectopically induce stomata beyond the epidermis. Development *140*, 1924-1935.

12. Casson, S.A., Franklin, K.A., Gray, J.E., Grierson, C.S., Whitelam, G.C., and Hetherington, A.M. (2009). phytochrome B and PIF4 regulate stomatal development in response to light quantity. Curr Biol *19*, 229-234.

13. Kang, C.Y., Lian, H.L., Wang, F.F., Huang, J.R., and Yang, H.Q. (2009). Cryptochromes, phytochromes, and COP1 regulate light-controlled stomatal development in Arabidopsis. Plant Cell *21*, 2624-2641.

14. Feng, P., Guo, H., Chi, W., Chai, X., Sun, X., Xu, X., Ma, J., Rochaix, J.-D., Leister, D., Wang, H., et al. (2016). Chloroplast retrograde signal regulates flowering. Proceedings of the National Academy of Sciences *113*, 10708-10713.

15. Petrillo, E., Godoy Herz, M.A., Fuchs, A., Reifer, D., Fuller, J., Yanovsky, M.J., Simpson, C., Brown, J.W., Barta, A., Kalyna, M., et al. (2014). A chloroplast retrograde signal regulates nuclear alternative splicing. Science *344*, 427-430.

16. Gray, G.R., Chauvin, L.P., Sarhan, F., and Huner, N. (1997). Cold Acclimation and Freezing Tolerance (A Complex Interaction of Light and Temperature). Plant Physiol *114*, 467-474.

17. Dickinson, P.J., Kumar, M., Martinho, C., Yoo, S.J., Lan, H., Artavanis, G., Charoensawan, V., Schöttler, M.A., Bock, R., Jaeger, K.E., et al. (2018). Chloroplast Signaling Gates Thermotolerance in Arabidopsis. Cell Rep *22*, 1657-1665.

18. Escoubas, J.M., Lomas, M., LaRoche, J., and Falkowski, P.G. (1995). Light intensity regulation of cab gene transcription is signaled by the redox state of the plastoquinone pool. Proceedings of the National Academy of Sciences of the United States of America *92*, 10237-10241.

19. Beemster, G.T., Fiorani, F., and Inzé, D. (2003). Cell cycle: the key to plant growth control? Trends Plant Sci *8*, 154-158.

20. Ohashi-Ito, K., and Bergmann, D.C. (2006). Arabidopsis FAMA controls the final proliferation/differentiation switch during stomatal development. Plant Cell *18*, 2493-2505.

21. Chamovitz, D., Pecker, I., and Hirschberg, J. (1991). The molecular basis of resistance to the herbicide norflurazon. Plant Mol Biol *16*, 967-974.

22. Bellafiore, S., Barneche, F., Peltier, G., and Rochaix, J.D. (2005). State transitions and light adaptation require chloroplast thylakoid protein kinase STN7. Nature *433*, 892-895.

23. Pribil, M., Pesaresi, P., Hertle, A., Barbato, R., and Leister, D. (2010). Role of Plastid Protein Phosphatase TAP38 in LHCII Dephosphorylation and Thylakoid Electron Flow. PLOS Biology *8*, e1000288.

24. Hepworth, C., Wood, W.H.J., Emrich-Mills, T.Z., Proctor, M.S., Casson, S., and Johnson, M.P. (2021). Dynamic thylakoid stacking and state transitions work synergistically to avoid acceptor-side limitation of photosystem I. Nat Plants *7*, 87-98.

25. Wood, W.H.J., MacGregor-Chatwin, C., Barnett, S.F.H., Mayneord, G.E., Huang, X., Hobbs, J.K., Hunter, C.N., and Johnson, M.P. (2018). Dynamic thylakoid stacking regulates the balance between linear and cyclic photosynthetic electron transfer. Nat Plants *4*, 116-127.

26. Hu, W., Franklin, K.A., Sharrock, R.A., Jones, M.A., Harmer, S.L., and Lagarias, J.C. (2013). Unanticipated regulatory roles for Arabidopsis phytochromes revealed by null mutant analysis. Proceedings of the National Academy of Sciences of the United States of America *110*, 1542-1547.

27. Lau, O.S., Davies, K.A., Chang, J., Adrian, J., Rowe, M.H., Ballenger, C.E., and Bergmann, D.C. (2014). Direct roles of SPEECHLESS in the specification of stomatal self-renewing cells. Science *345*, 1605.

28. Hunt, L., Bailey, K.J., and Gray, J.E. (2010). The signalling peptide EPFL9 is a positive regulator of stomatal development. New Phytol. *186*, 609-614.

29. Charuvi, D., Kiss, V., Nevo, R., Shimoni, E., Adam, Z., and Reich, Z. (2012). Gain and Loss of Photosynthetic Membranes during Plastid Differentiation in the Shoot Apex of Arabidopsis The Plant Cell *24*, 1143-1157.

30. Wang, P., Du, Y., Li, Y., Ren, D., and Song, C.-P. (2010). Hydrogen peroxide-mediated activation of MAP kinase 6 modulates nitric oxide biosynthesis and signal transduction in Arabidopsis. The Plant cell *22*, 2981-2998.

31. Lokdarshi, A., Guan, J., Urquidi Camacho, R.A., Cho, S.K., Morgan, P.W., Leonard, M., Shimono, M., Day, B., and von Arnim, A.G. (2020). Light Activates the Translational Regulatory Kinase GCN2 via Reactive Oxygen Species Emanating from the Chloroplast. Plant Cell *32*, 1161-1178.

32. Ruckle, M.E., DeMarco, S.M., and Larkin, R.M. (2007). Plastid Signals Remodel Light Signaling Networks and Are Essential for Efficient Chloroplast Biogenesis in Arabidopsis. The Plant Cell *19*, 3944-3960.

33. Guo, H., Feng, P., Chi, W., Sun, X., Xu, X., Li, Y., Ren, D., Lu, C., David Rochaix, J., Leister, D., et al. (2016). Plastid-nucleus communication involves calcium-modulated MAPK signalling. Nat. Commun. *7*, 12173.

34. Puthiyaveetil, S., Kavanagh, T.A., Cain, P., Sullivan, J.A., Newell, C.A., Gray, J.C., Robinson, C., van der Giezen, M., Rogers, M.B., and Allen, J.F. (2008). The ancestral symbiont sensor kinase CSK links photosynthesis with gene expression in chloroplasts. Proc Natl Acad Sci U S A *105*, 10061-10066.

35. Lau, O.S., Song, Z., Zhou, Z., Davies, K.A., Chang, J., Yang, X., Wang, S., Lucyshyn, D., Tay, I.H.Z., Wigge, P.A., et al. (2018). Direct Control of SPEECHLESS by PIF4 in the High-Temperature Response of Stomatal Development. Curr Biol *28*, 1273-1280.e1273.

36. Abe, M., Takahashi, T., and Komeda, Y. (2001). Identification of a cis-regulatory element for L1 layer-specific gene expression, which is targeted by an L1-specific homeodomain protein. Plant J *26*, 487-494.

37. Li, H., Ding, Y., Shi, Y., Zhang, X., Zhang, S., Gong, Z., and Yang, S. (2017). MPK3- and MPK6-Mediated ICE1 Phosphorylation Negatively Regulates ICE1 Stability and Freezing Tolerance in Arabidopsis. Dev Cell *43*, 630-642.e634.

38. Rosso, D., Bode, R., Li, W., Krol, M., Saccon, D., Wang, S., Schillaci, L.A., Rodermel, S.R., Maxwell, D.P., and Hüner, N.P.A. (2009). Photosynthetic redox imbalance governs leaf sectoring in the Arabidopsis thaliana variegation mutants immutans, spotty, var1, and var2. The Plant cell *21*, 3473-3492.

39. Wilson, K.E.W.E., Ivanov, A.G.I.G., Öquist, G., Grodzinski, B., Sarhan, F., and Huner, N.P.A.H.P.A. (2006). Energy balance, organellar redox status, and acclimation to environmental stress. Canadian Journal of Botany *84*, 1355-1370.

40. Engineer, C.B., Ghassemian, M., Anderson, J.C., Peck, S.C., Hu, H., and Schroeder, J.I. (2014). Carbonic anhydrases, EPF2 and a novel protease mediate CO(2) control of stomatal development. Nature *513*, 246-250.

41. Bolte, S., and Cordelières, F.P. (2006). A guided tour into subcellular colocalization analysis in light microscopy. J Microsc *224*, 213-232.

42. Merkouropoulos, G., Andreasson, E., Hess, D., Boller, T., and Peck, S.C. (2008). An Arabidopsis protein phosphorylated in response to microbial elicitation, AtPHOS32, is a substrate of MAP kinases 3 and 6. J Biol Chem *283*, 10493-10499.

43. Nakamura, M., Katsumata, H., Abe, M., Yabe, N., Komeda, Y., Yamamoto, K.T., and Takahashi, T. (2006). Characterization of the class IV homeodomain-Leucine Zipper gene family in Arabidopsis. Plant Physiol *141*, 1363-1375.

44. Lorrain, S., Allen, T., Duek, P.D., Whitelam, G.C., and Fankhauser, C. (2008). Phytochrome-mediated inhibition of shade avoidance involves degradation of growth-promoting bHLH transcription factors. Plant J *53*, 312-323.

45. Czechowski, T., Stitt, M., Altmann, T., Udvardi, M.K., and Scheible, W.-R. (2005). Genome-wide identification and testing of superior reference genes for transcript normalization in Arabidopsis. Plant physiology *139*, 5-17.

46. Livak, K.J., and Schmittgen, T.D. (2001). Analysis of relative gene expression data using real-time quantitative PCR and the 2(-Delta Delta C(T)) Method. Methods *25*, 402-408.

47. Schindelin, J., Arganda-Carreras, I., Frise, E., Kaynig, V., Longair, M., Pietzsch, T., Preibisch, S., Rueden, C., Saalfeld, S., Schmid, B., et al. (2012). Fiji: an open-source platform for biological-image analysis. Nat Methods *9*, 676-682.

48. Linkert, M., Rueden, C.T., Allan, C., Burel, J.-M., Moore, W., Patterson, A., Loranger, B., Moore, J., Neves, C., MacDonald, D., et al. (2010). Metadata matters: access to image data in the real world. Journal of Cell Biology *189*, 777-782.

49. Zoulias, N., Brown, J., Rowe, J., and Casson, S.A. (2020). HY5 is not integral to light mediated stomatal development in Arabidopsis. PLOS ONE *15*, e0222480.

50. Zhong, S., Lin, Z., Fray, R.G., and Grierson, D. (2008). Improved plant transformation vectors for fluorescent protein tagging. Transgenic Res *17*, 985-989.

51. Brand, L., Hörler, M., Nüesch, E., Vassalli, S., Barrell, P., Yang, W., Jefferson, R.A., Grossniklaus, U., and Curtis, M.D. (2006). A versatile and reliable two-component system for tissue-specific gene induction in Arabidopsis. Plant Physiol *141*, 1194-1204.

52. Benfey, P.N., Ren, L., and Chua, N.H. (1989). The CaMV 35S enhancer contains at least two domains which can confer different developmental and tissue-specific expression patterns. EMBO J *8*, 2195-2202.

53. Curtis, M.D., and Grossniklaus, U. (2003). A Gateway Cloning Vector Set for High-Throughput Functional Analysis of Genes in Planta. Plant Physiology *133*, 462-469.

54. Clough, S.J., and Bent, A.F. (1998). Floral dip: a simplified method for Agrobacterium-mediated transformation of Arabidopsis thaliana. Plant J *16*, 735-743.

55. Wu, F.-H., Shen, S.-C., Lee, L.-Y., Lee, S.-H., Chan, M.-T., and Lin, C.-S. (2009). Tape-Arabidopsis Sandwich - a simpler Arabidopsis protoplast isolation method. Plant Methods *5*, 16.

56. Hellens, R.P., Allan, A.C., Friel, E.N., Bolitho, K., Grafton, K., Templeton, M.D., Karunairetnam, S., Gleave, A.P., and Laing, W.A. (2005). Transient expression vectors for functional genomics, quantification of promoter activity and RNA silencing in plants. Plant Methods *1*, 13-13.

57. Flury, P., Klauser, D., Boller, T., and Bartels, S. (2013). MAPK Phosphorylation Assay with Leaf Disks of Arabidopsis. Bio-protocol *3*, e929.

58. Flury, P., Klauser, D., Schulze, B., Boller, T., and Bartels, S. (2013). The anticipation of danger: microbe-associated molecular pattern perception enhances AtPep-triggered oxidative burst. Plant physiology *161*, 2023-2035.

59. Millson, S.H., Truman, A.W., and Piper, P.W. (2003). Vectors for N- or C-terminal positioning of the yeast Gal4p DNA binding or activator domains. Biotechniques *35*, 60-64.

60. Gietz, R.D., and Woods, R.A. (2002). Transformation of yeast by lithium acetate/single-stranded carrier DNA/polyethylene glycol method. Methods Enzymol *350*, 87-96.

61. James, P., Halladay, J., and Craig, E.A. (1996). Genomic libraries and a host strain designed for highly efficient two-hybrid selection in yeast. Genetics *144*, 1425-1436.

62. Chastanet, A., Fert, J., and Msadek, T. (2003). Comparative genomics reveal novel heat shock regulatory mechanisms in Staphylococcus aureus and other Gram-positive bacteria. Mol Microbiol *47*, 1061-1073.

Figure 1

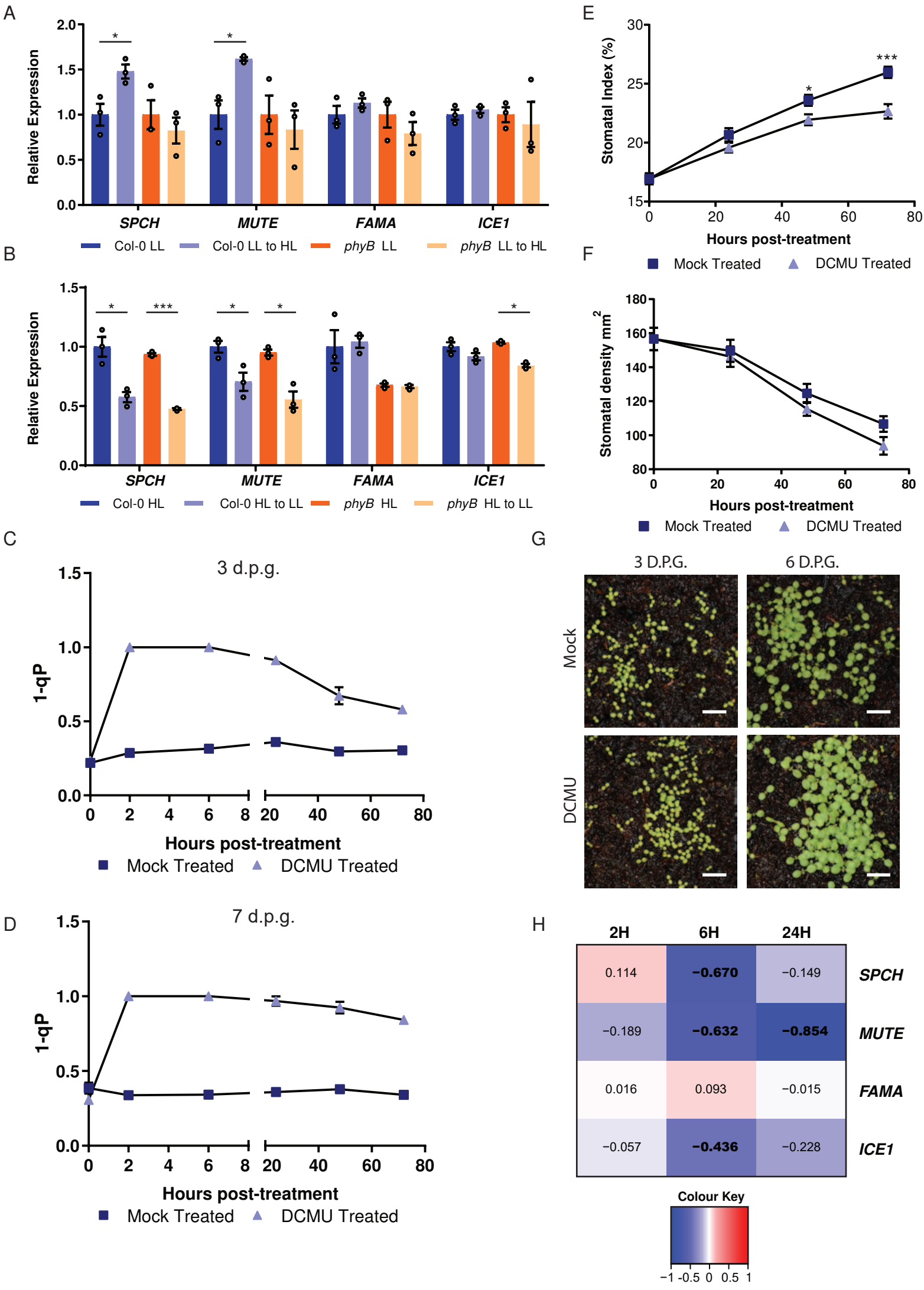
A
Relative Expression
2.0
1.5
1.0
0.5
0.0
*
*
SPCH
MUTE
FAMA
ICE1
Col-0 LL
Col-0 LL to HL
phyB LL
phyB LL to HL
B
Relative Expression
1.5
1.0
0.5
0.0
*
***
*
*
*
SPCH
MUTE
FAMA
ICE1
Col-0 HL
Col-0 HL to LL
phyB HL
phyB HL to LL
C
3 d.p.g.
1-qP
1.5
1.0
0.5
0.0
0
2
4
6
8
20
40
60
80
Hours post-treatment
Mock Treated
DCMU Treated
D
7 d.p.g.
1-qP
1.5
1.0
0.5
0.0
0
2
4
6
8
20
40
60
80
Hours post-treatment
Mock Treated
DCMU Treated
E
Stomatal Index (%)
30
25
20
15
*
***
0
20
40
60
80
Hours post-treatment
Mock Treated
DCMU Treated
F
Stomatal density mm2
180
160
140
120
100
80
0
20
40
60
80
Hours post-treatment
Mock Treated
DCMU Treated
G
3 D.P.G.
6 D.P.G.
Mock
DCMU
H
2H
6H
24H
0.114
−0.670
−0.149
SPCH
−0.189
−0.632
−0.854
MUTE
0.016
0.093
−0.015
FAMA
−0.057
−0.436
−0.228
ICE1
Colour Key
−1 -0.5 0 0.5 1

# Figure S1

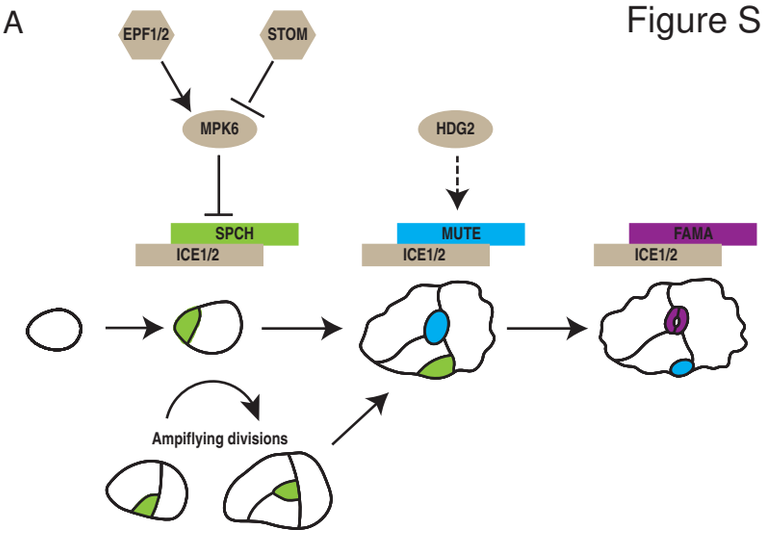
A
EPF1/2
STOM
MPK6
HDG2
SPCH
ICE1/2
MUTE
ICE1/2
FAMA
ICE1/2
Ampiflying divisions

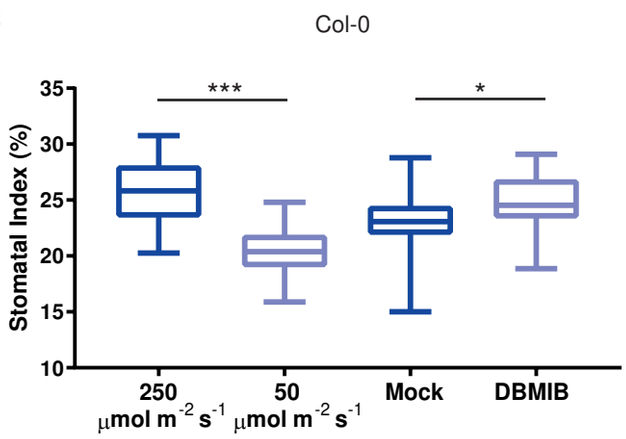
B
Col-0
Stomatal Index (%)
***
*
250 µmol m-2 s-1
50 µmol m-2 s-1
Mock
DBMIB

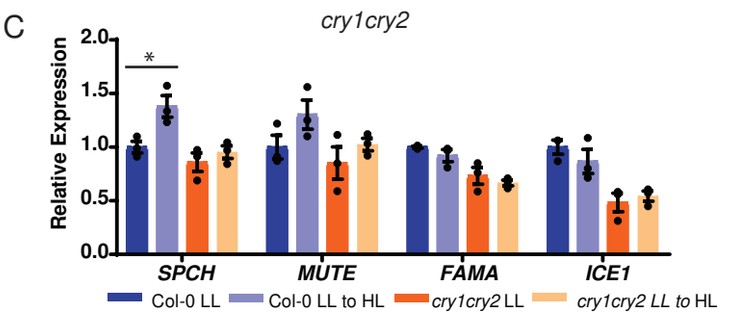
C
cry1cry2
Relative Expression
SPCH
MUTE
FAMA
ICE1
Col-0 LL
Col-0 LL to HL
cry1cry2 LL
cry1cry2 LL to HL

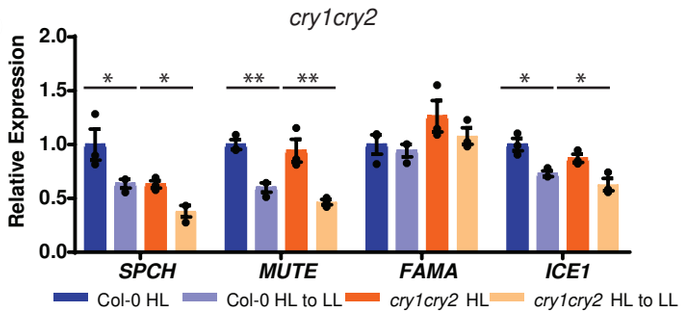
D
cry1cry2
Relative Expression
SPCH
MUTE
FAMA
ICE1
Col-0 HL
Col-0 HL to LL
cry1cry2 HL
cry1cry2 HL to LL

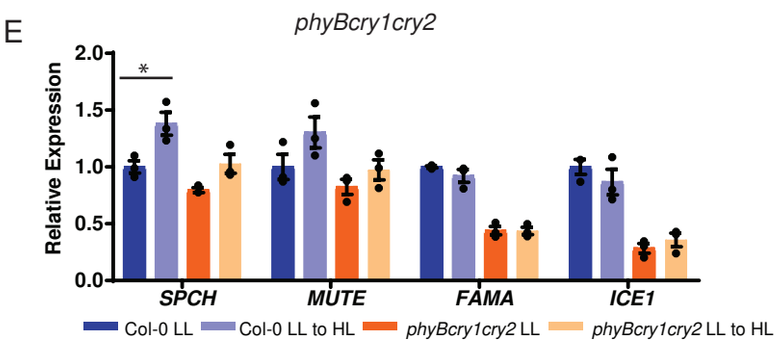
E
phyBcry1cry2
Relative Expression
SPCH
MUTE
FAMA
ICE1
Col-0 LL
Col-0 LL to HL
phyBcry1cry2 LL
phyBcry1cry2 LL to HL

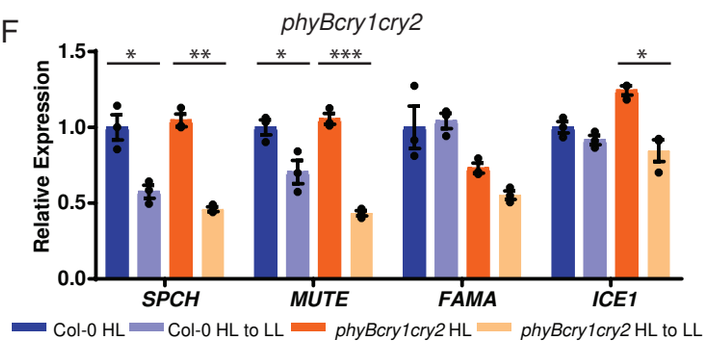
F
phyBcry1cry2
Relative Expression
SPCH
MUTE
FAMA
ICE1
Col-0 HL
Col-0 HL to LL
phyBcry1cry2 HL
phyBcry1cry2 HL to LL

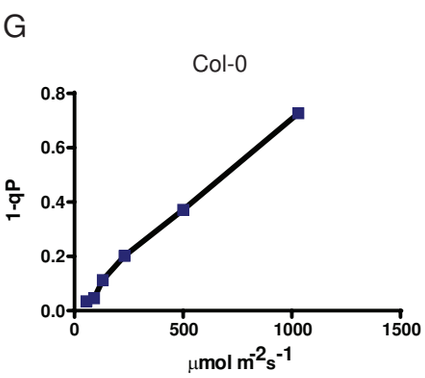
G
Col-0
1-qP
µmol m-2s-1

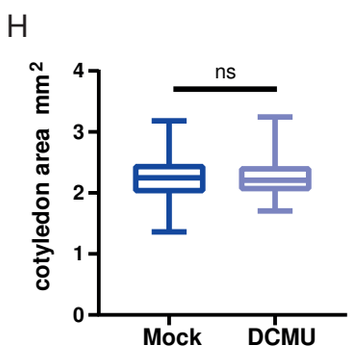
H
ns
cotyledon area mm2
Mock
DCMU

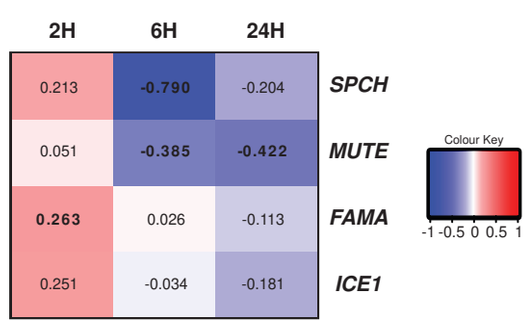
I
2H
6H
24H
0.213
-0.790
-0.204
SPCH
0.051
-0.385
-0.422
MUTE
0.263
0.026
-0.113
FAMA
0.251
-0.034
-0.181
ICE1
Colour Key
-1 -0.5 0 0.5 1

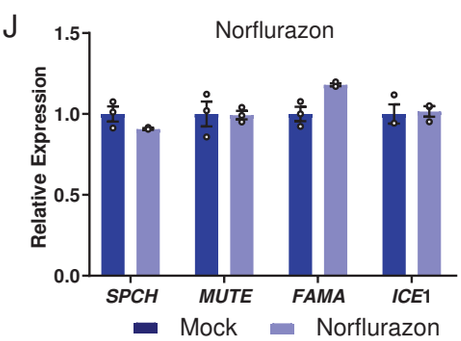
J
Norflurazon
Relative Expression
SPCH
MUTE
FAMA
ICE1
Mock
Norflurazon

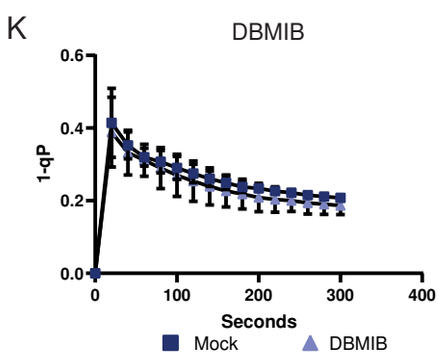
K
DBMIB
1-qP
Seconds
Mock
DBMIB

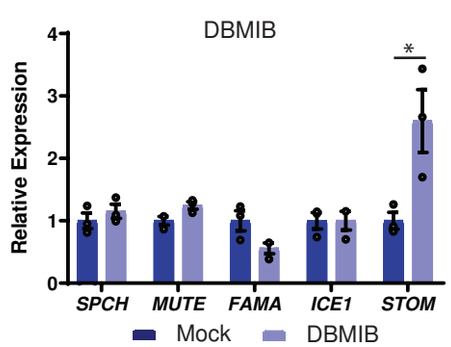
L
DBMIB
Relative Expression
SPCH
MUTE
FAMA
ICE1
STOM
Mock
DBMIB

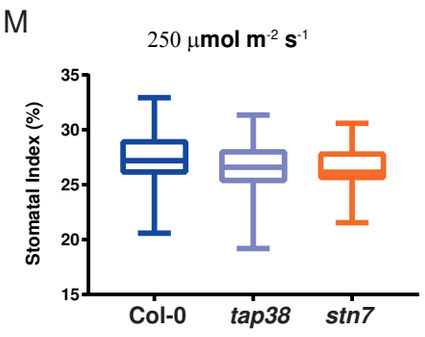
M
250 µmol m-2 s-1
Stomatal Index (%)
Col-0
tap38
stn7

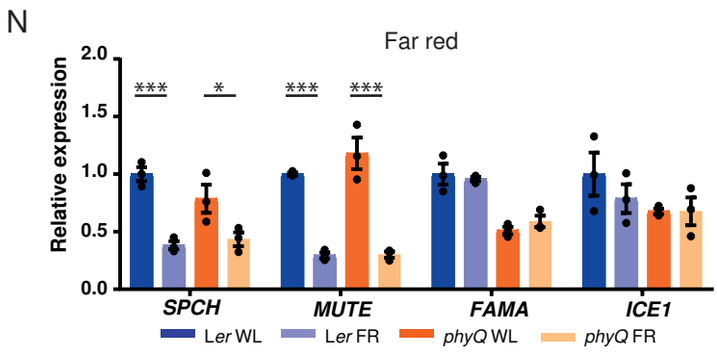
N
Far red
Relative expression
SPCH
MUTE
FAMA
ICE1
Ler WL
Ler FR
phyQ WL
phyQ FR

Figure 2

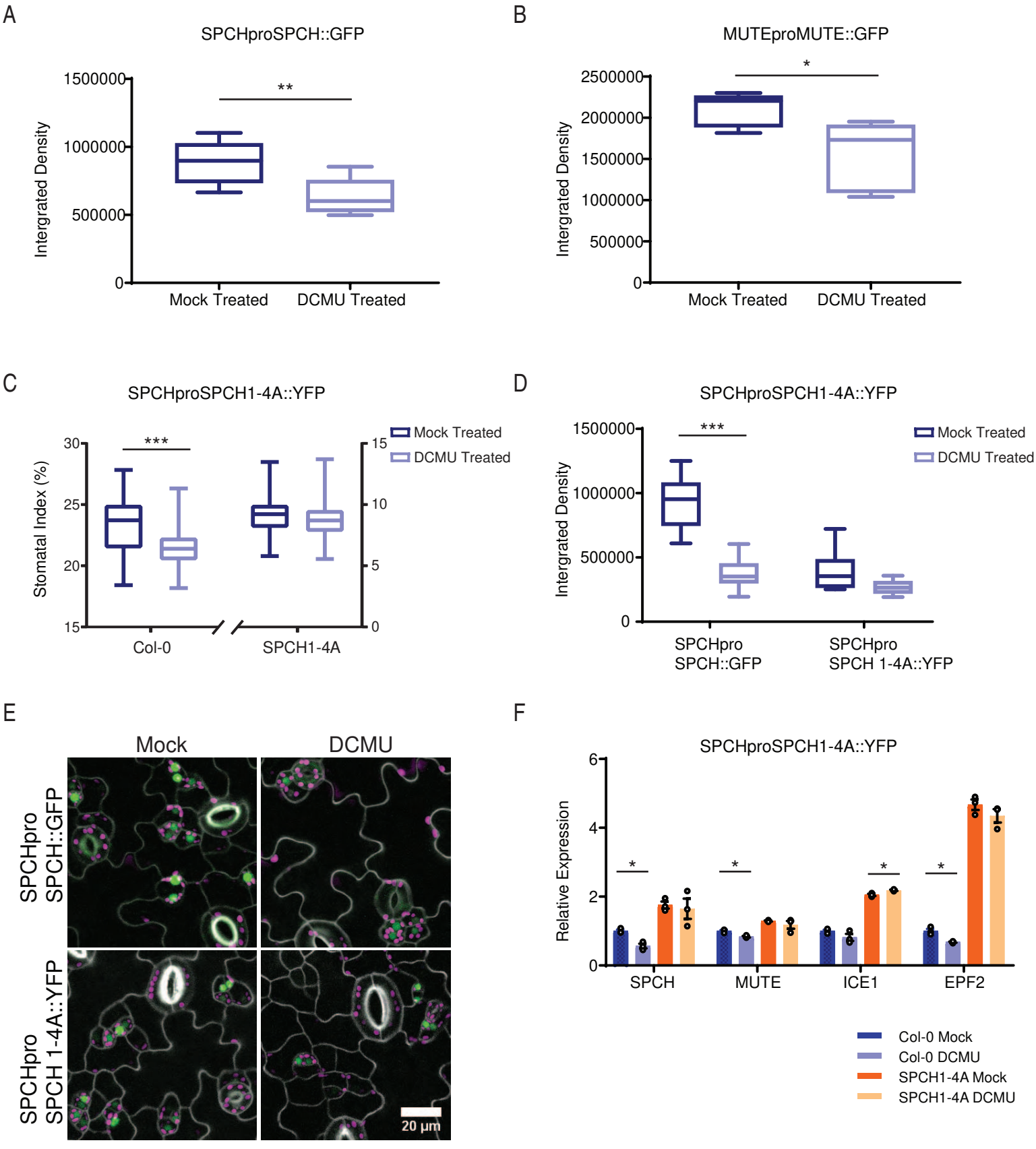
A
SPCHproSPCH::GFP
Intergrated Density
1500000
1000000
500000
0
**
Mock Treated
DCMU Treated
B
MUTEproMUTE::GFP
Intergrated Density
2500000
2000000
1500000
1000000
500000
0
*
Mock Treated
DCMU Treated
C
SPCHproSPCH1-4A::YFP
Stomatal Index (%)
30
25
20
15
15
10
5
0
***
Mock Treated
DCMU Treated
Col-0
SPCH1-4A
D
SPCHproSPCH1-4A::YFP
Intergrated Density
1500000
1000000
500000
0
***
Mock Treated
DCMU Treated
SPCHpro SPCH::GFP
SPCHpro SPCH 1-4A::YFP
E
Mock
DCMU
SPCHpro SPCH::GFP
SPCHpro SPCH 1-4A::YFP
20 µm
F
SPCHproSPCH1-4A::YFP
Relative Expression
6
4
2
0
*
SPCH
MUTE
ICE1
EPF2
Col-0 Mock
Col-0 DCMU
SPCH1-4A Mock
SPCH1-4A DCMU

Figure S2

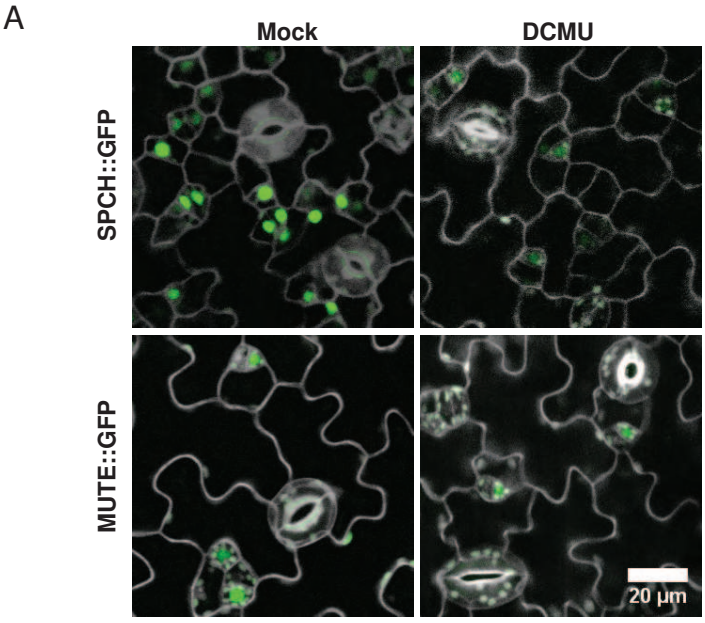


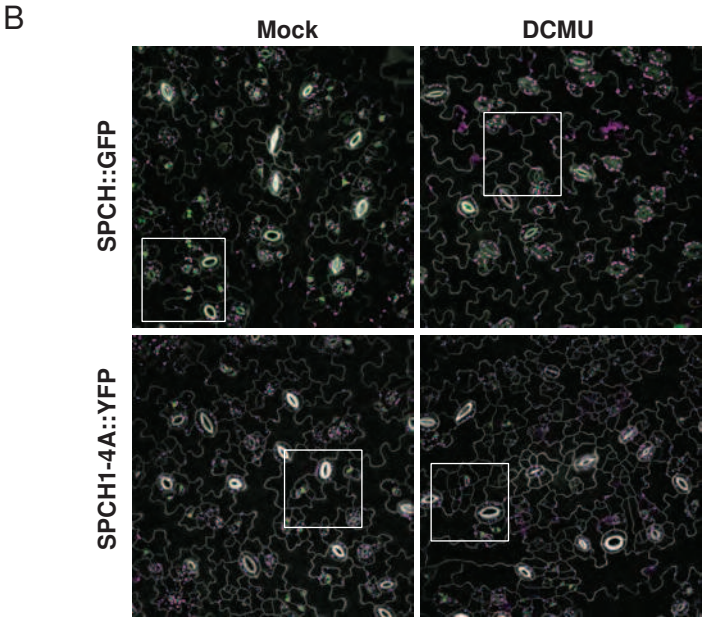


Original (uncropped) pictures of Fig. 2E

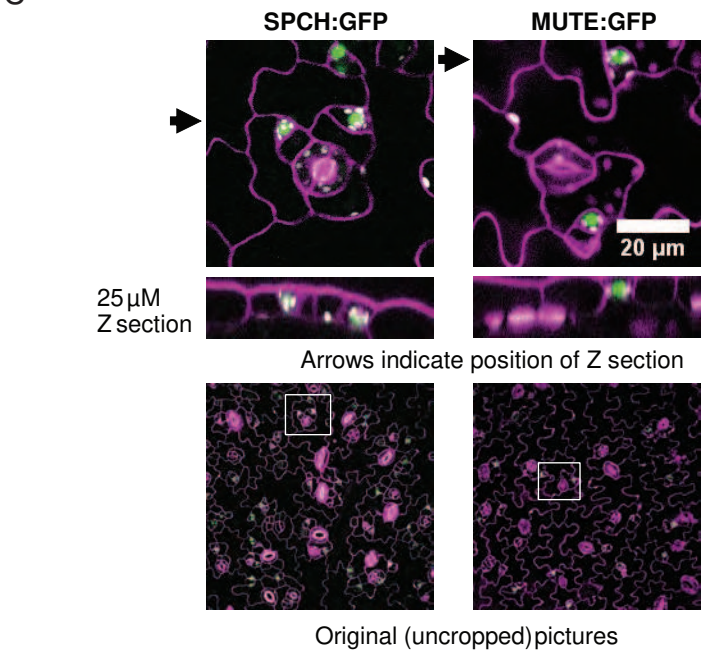


Arrows indicate position of Z section

Original (uncropped) pictures

Figure 3

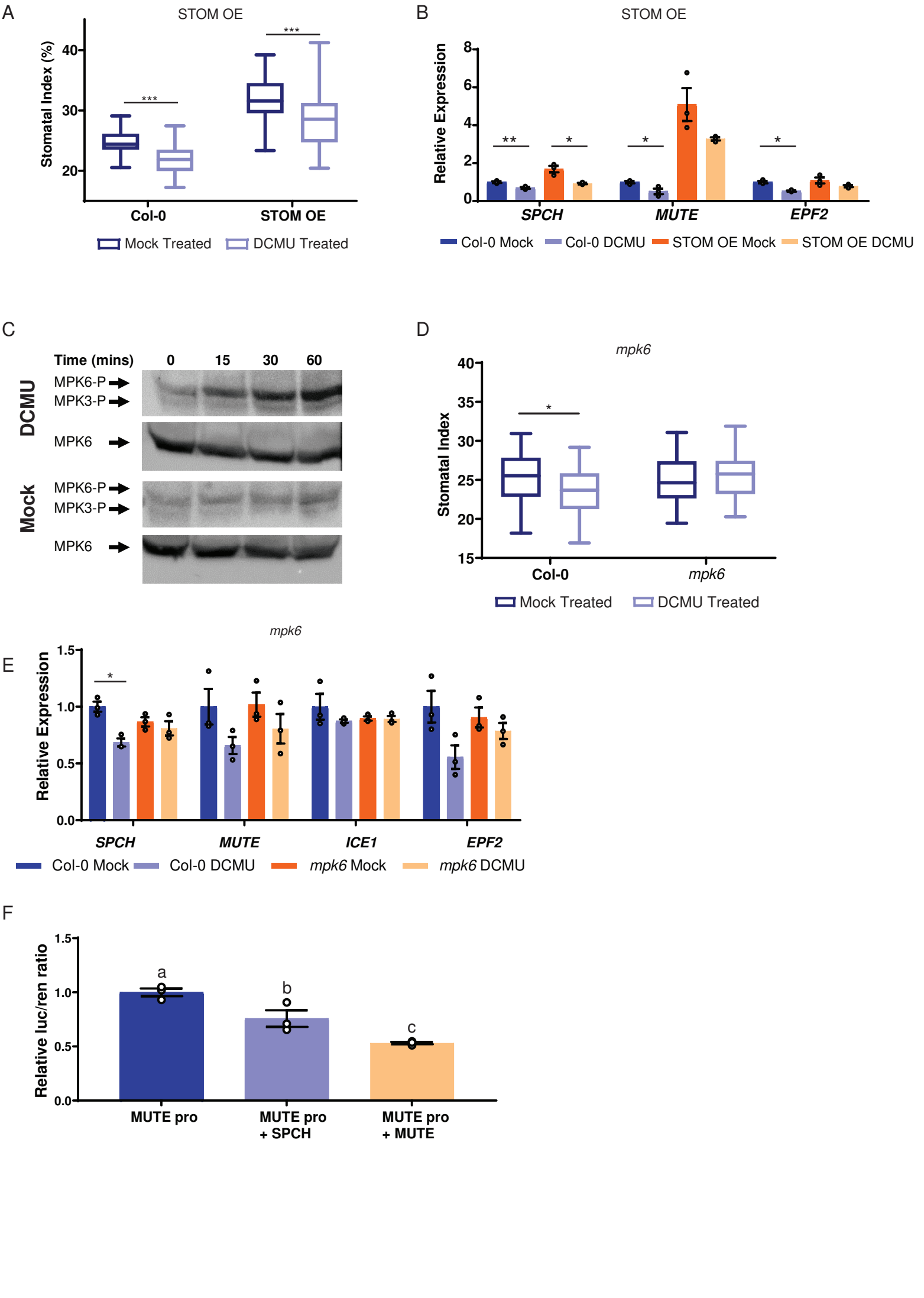
A
STOM OE
Stomatal Index (%)
40
30
20
***
***
Col-0
STOM OE
Mock Treated
DCMU Treated
B
STOM OE
Relative Expression
8
6
4
2
0
**
*
*
*
SPCH
MUTE
EPF2
Col-0 Mock
Col-0 DCMU
STOM OE Mock
STOM OE DCMU
C
Time (mins)
0
15
30
60
DCMU
MPK6-P
MPK3-P
MPK6
Mock
MPK6-P
MPK3-P
MPK6
D
mpk6
Stomatal Index
40
35
30
25
20
15
*
Col-0
mpk6
Mock Treated
DCMU Treated
E
mpk6
Relative Expression
1.5
1.0
0.5
0.0
*
SPCH
MUTE
ICE1
EPF2
Col-0 Mock
Col-0 DCMU
mpk6 Mock
mpk6 DCMU
F
Relative luc/ren ratio
1.5
1.0
0.5
0.0
a
b
c
MUTE pro
MUTE pro
+ SPCH
MUTE pro
+ MUTE

Figure S3

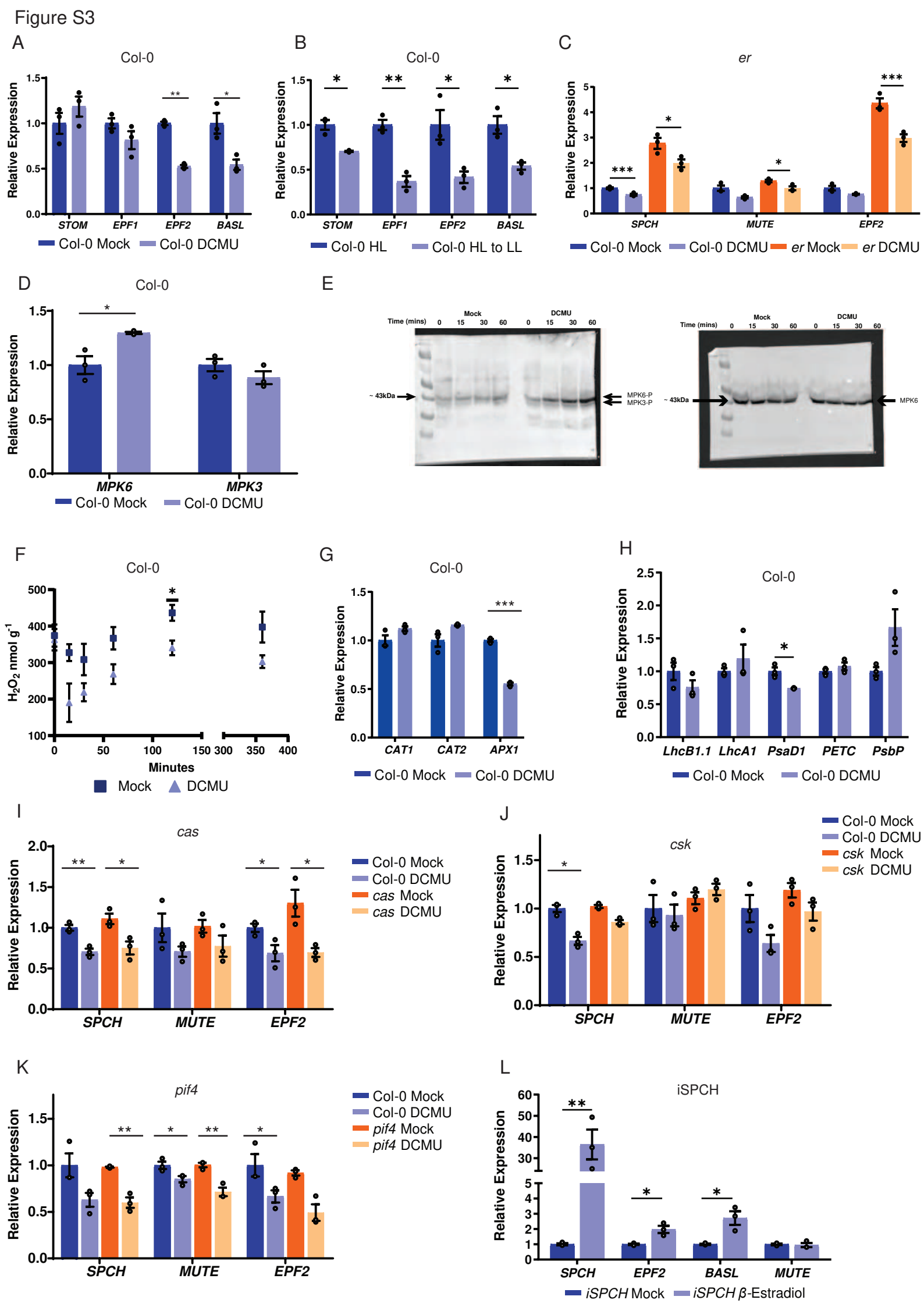
A
Col-0
Relative Expression
STOM
EPF1
EPF2
BASL
Col-0 Mock
Col-0 DCMU
B
Col-0
Relative Expression
STOM
EPF1
EPF2
BASL
Col-0 HL
Col-0 HL to LL
C
er
Relative Expression
SPCH
MUTE
EPF2
Col-0 Mock
Col-0 DCMU
er Mock
er DCMU
D
Col-0
Relative Expression
MPK6
MPK3
Col-0 Mock
Col-0 DCMU
E
Mock
DCMU
Time (mins) 0 15 30 60 0 15 30 60
~ 43kDa
MPK6-P
MPK3-P
MPK6
F
Col-0
H2O2 nmol g-1
Minutes
Mock
DCMU
G
Col-0
Relative Expression
CAT1
CAT2
APX1
Col-0 Mock
Col-0 DCMU
H
Col-0
Relative Expression
LhcB1.1
LhcA1
PsaD1
PETC
PsbP
Col-0 Mock
Col-0 DCMU
I
cas
Relative Expression
SPCH
MUTE
EPF2
Col-0 Mock
Col-0 DCMU
cas Mock
cas DCMU
J
csk
Relative Expression
SPCH
MUTE
EPF2
Col-0 Mock
Col-0 DCMU
csk Mock
csk DCMU
K
pif4
Relative Expression
SPCH
MUTE
EPF2
Col-0 Mock
Col-0 DCMU
pif4 Mock
pif4 DCMU
L
iSPCH
Relative Expression
SPCH
EPF2
BASL
MUTE
iSPCH Mock
iSPCH β-Estradiol

Figure 4

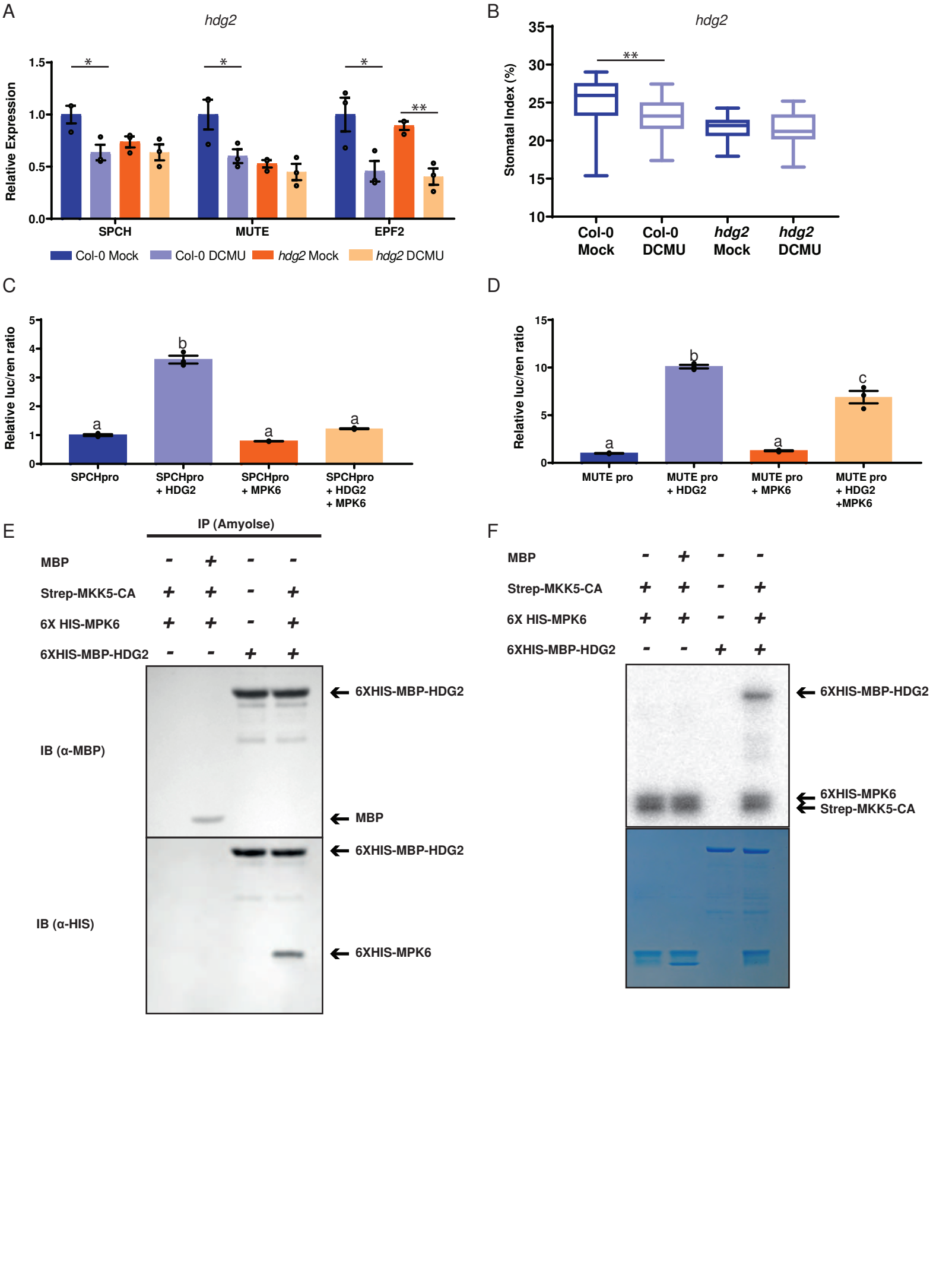
A
hdg2
Relative Expression
1.5
1.0
0.5
0.0
*
*
*
**
SPCH
MUTE
EPF2
Col-0 Mock
Col-0 DCMU
hdg2 Mock
hdg2 DCMU
B
hdg2
Stomatal Index (%)
35
30
25
20
15
10
**
Col-0 Mock
Col-0 DCMU
hdg2 Mock
hdg2 DCMU
C
Relative luc/ren ratio
5
4
3
2
1
0
a
b
a
a
SPCHpro
SPCHpro + HDG2
SPCHpro + MPK6
SPCHpro + HDG2 + MPK6
D
Relative luc/ren ratio
15
10
5
0
a
b
a
c
MUTE pro
MUTE pro + HDG2
MUTE pro + MPK6
MUTE pro + HDG2 +MPK6
E
IP (Amyolse)
MBP - + - -
Strep-MKK5-CA + + - +
6X HIS-MPK6 + + - +
6XHIS-MBP-HDG2 - - + +
IB (α-MBP)
6XHIS-MBP-HDG2
MBP
IB (α-HIS)
6XHIS-MBP-HDG2
6XHIS-MPK6
F
MBP - + - -
Strep-MKK5-CA + + - +
6X HIS-MPK6 + + - +
6XHIS-MBP-HDG2 - - + +
6XHIS-MBP-HDG2
6XHIS-MPK6
Strep-MKK5-CA

Figure S4

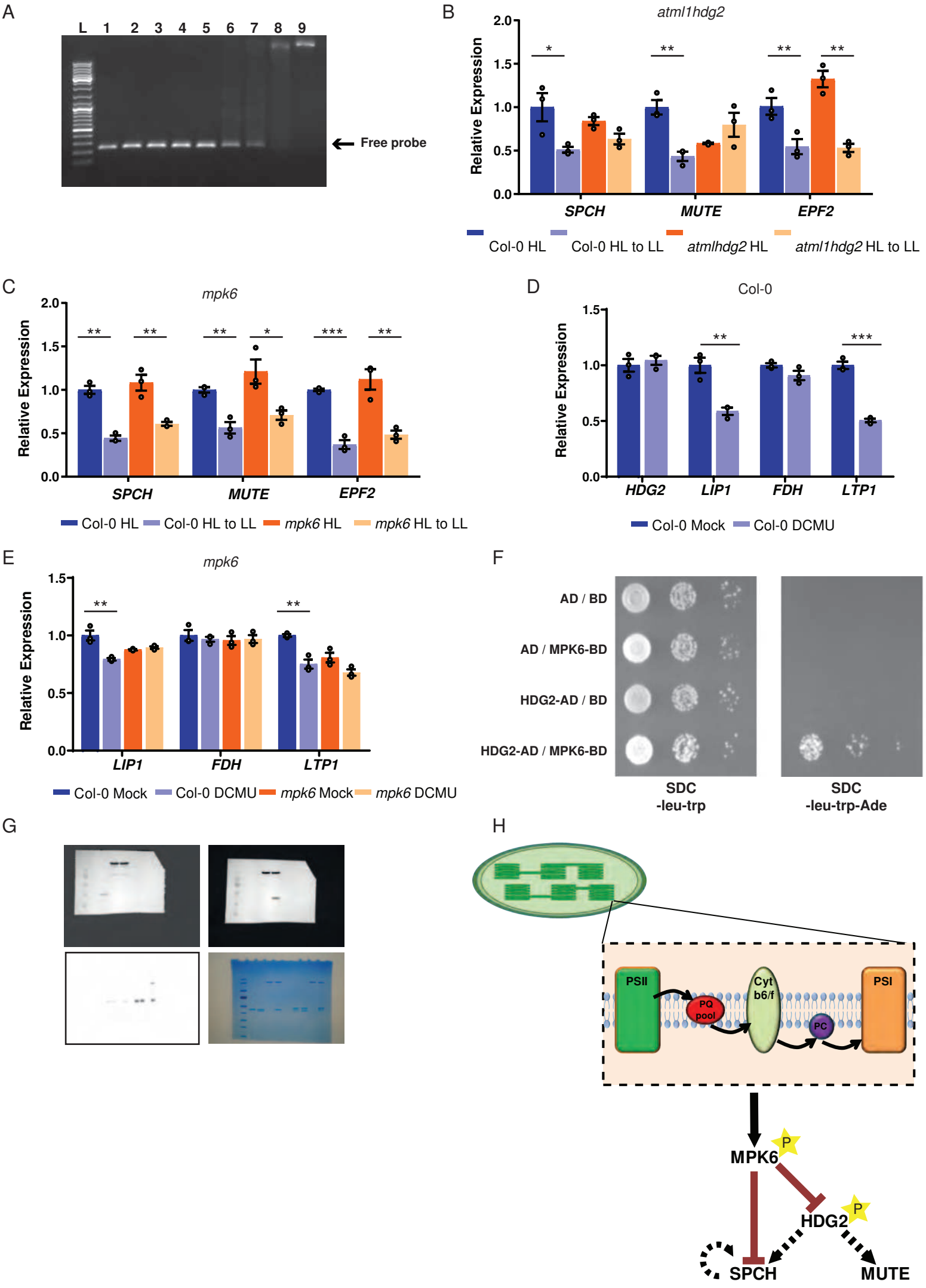
A
L 1 2 3 4 5 6 7 8 9
Free probe
B
atml1hdg2
Relative Expression
SPCH
MUTE
EPF2
Col-0 HL
Col-0 HL to LL
atmlhdg2 HL
atml1hdg2 HL to LL
C
mpk6
Relative Expression
SPCH
MUTE
EPF2
Col-0 HL
Col-0 HL to LL
mpk6 HL
mpk6 HL to LL
D
Col-0
Relative Expression
HDG2
LIP1
FDH
LTP1
Col-0 Mock
Col-0 DCMU
E
mpk6
Relative Expression
LIP1
FDH
LTP1
Col-0 Mock
Col-0 DCMU
mpk6 Mock
mpk6 DCMU
F
AD / BD
AD / MPK6-BD
HDG2-AD / BD
HDG2-AD / MPK6-BD
SDC
-leu-trp
SDC
-leu-trp-Ade
G
H
PSII
PQ pool
Cyt b6/f
PC
PSI
MPK6
P
HDG2
P
SPCH
MUTE